AD-A067 845 HARRY DIAMOND LABS ADELPHI MD F/G 7/2
ENERGY LEVELS AND LINE INTENSITIES FOR THE GROUND CONFIGURATION--ETC(U)
FEB 79 L ESTEROWITZ, F J BARTOLI, R E ALLEN
UNCLASSIFIED HDL-TR-1875 NL

| OF |
AD
A067845

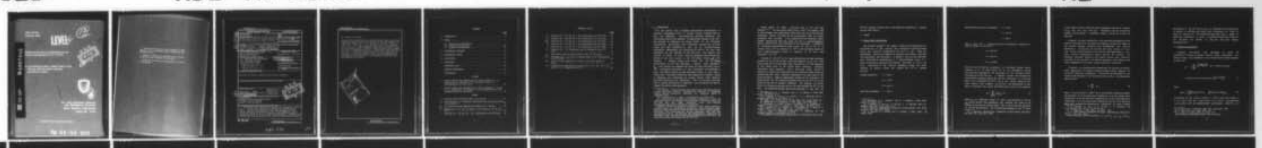

END
DATE
FILMED
6-79
DDC

HDL-TR-1875
February 1979

LEVEL II

12 VU

Energy Levels and Line Intensities for the Ground Configuration of Pr^{3+} in $LiYF_4$

by Leon Esterowitz, Filbert J. Bartoli, Roger E. Allen, Donald E. Wortman, Clyde A. Morrison, and Richard P. Leavitt

U.S. Army Electronics Research and Development Command
Harry Diamond Laboratories
Adelphi, MD 20783

The findings in this report are not to be construed as an official Department of the Army position unless so designated by other authorized documents.

Citation of manufacturers' or trade names does not constitute an official indorsement or approval of the use thereof.

Destroy this report when it is no longer needed. Do not return it to the originator.

UNCLASSIFIED
SECURITY CLASSIFICATION OF THIS PAGE (When Date Entered)

REPORT DOCUMENTATION PAGE

READ INSTRUCTIONS BEFORE COMPLETING FORM

1. REPORT NUMBER: HDL-TR-1875	2. GOVT ACCESSION NO.
3. RECIPIENT'S CATALOG NUMBER	
4. TITLE (and Subtitle): Energy Levels and Line Intensities for the Ground Configuration of Pr^{3+} in $LiYF_4$	5. TYPE OF REPORT & PERIOD COVERED: Technical Report
	6. PERFORMING ORG. REPORT NUMBER
7. AUTHOR(s): Leon Esterowitz, Filbert J. Bartoli, Roger E. Allen, Donald E. Wortman, Clyde A. Morrison, Richard P. Leavitt	8. CONTRACT OR GRANT NUMBER(s)
9. PERFORMING ORGANIZATION NAME AND ADDRESS: Harry Diamond Laboratories, 2800 Powder Mill Road, Adelphi, MD 20783	10. PROGRAM ELEMENT, PROJECT, TASK AREA & WORK UNIT NUMBERS: Program Ele: 6.11.02A
11. CONTROLLING OFFICE NAME AND ADDRESS: U.S. Army Materiel Development and Readiness Command, 5001 Eisenhower, Avenue, Alexandria, VA 22333	12. REPORT DATE: February 1979
	13. NUMBER OF PAGES: 55
	15. SECURITY CLASS. (of this report): Unclassified
	15a. DECLASSIFICATION/DOWNGRADING SCHEDULE

16. DISTRIBUTION STATEMENT (of this Report)

Approved for public release; distribution unlimited.

17. DISTRIBUTION STATEMENT (of the abstract entered in Block 20, if different from Report)

18. SUPPLEMENTARY NOTES

HDL Project: 308837
DRCMS Code: 611102.H.46H111
DA: 1L161102AH46H1

19. KEY WORDS (Continue on reverse side if necessary and identify by block number)

Praseodymium
Absorption and fluorescent spectra
Lithium yttrium fluoride
Crystal field parameters

20. ABSTRACT (Continue on reverse side if necessary and identify by block number)

High-resolution polarized absorption and fluorescence spectra of Pr^{3+} in $LiYF_4$ were measured at temperatures between 10 and 300 K. Energy level assignments were made assuming electric dipole transition selection rules for S_4 site symmetry. Forty-six energy levels of the $4f^2$ ground configuration were established, including 44 in the lowest nine multiplets. Crystal field calculations were performed by two different theoretical methods.

DD FORM 1 JAN 73 1473

UNCLASSIFIED
SECURITY CLASSIFICATION OF THIS PAGE (When Date Entered)

20. Abstract (Cont'd)

Crystal field parameters were determined that give a root mean square deviation of 15.8 cm^{-1} among 41 of the experimental and calculated energy values. The parameters are B_{20} = 488.9, B_{40} = -1043, B_{44} = 1242, B_{60} = -42, real B_{64} = 1213, and imaginary B_{64} = 22.5 cm^{-1}. These parameters were used to obtain the remaining energy levels, yielding a complete energy level scheme for the $4f^2$ configuration of Pr^{3+}. The crystal field parameters for Pr^{3+} in $LiYF_4$ were compared with those for other ions in this host. A theoretical calculation of line intensities was performed in which the oddfold crystal field parameters were obtained from a lattice sum. Line intensities were measured and compared with theory.

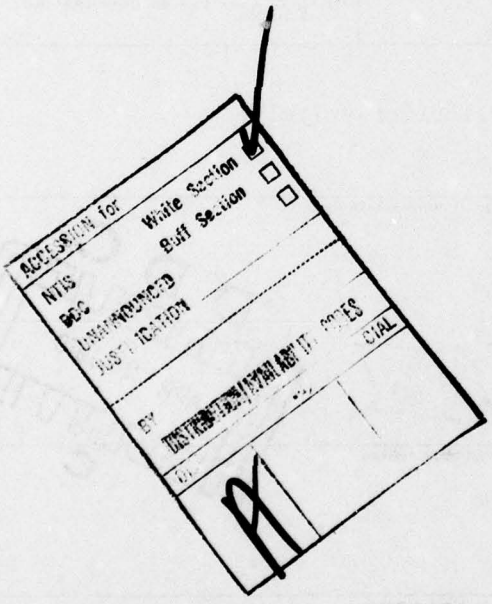

CONTENTS

FIGURES

TABLES

CONTENTS (Cont'd)

1. INTRODUCTION

In the present work, a systematic spectroscopic investigation of trivalent praseodymium (Pr^{3+}) in lithium yttrium fluoride ($LiYF_4$ or YLF) was undertaken. High-resolution polarized absorption and fluorescence spectra were measured at temperatures between 10 and 300 K and analyzed to determine the energy levels of the $4f^2$ ground configuration. Spectroscopic data previously reported for Pr^{3+}:YLF either have been incomplete[1] or have led to incorrect[2] energy assignments. Experimental line intensities for Pr^{3+} in YLF also were determined and are reported for the first time. The spectra were analyzed in detail to obtain empirical parameters that describe the effects of the host lattice on the Pr^{3+} energy levels. In this analysis, a complete energy level scheme for the $4f^2$ ground configuration of Pr^{3+} was determined. Crystal field parameters, B_{kq}, were obtained and compared with those for other rare-earth ions in YLF. A theoretical calculation of line intensities was performed in which the oddfold (odd-k) B_{kq} were determined ahead of time from a lattice sum. Calculated intensities were compared with measured values to determine the limitations* of current crystal field theory in accurately predicting line intensities. This is the first time that such a rigorous calculation† of individual line intensities was used to compare calculation with experiment.

---

[1] *H.P. Jenssen, Phonon Assisted Laser Transitions and Energy Transfer in Rare Earth Laser Crystals, Massachusetts Institute of Technology Crystal Physics Laboratory, Cambridge, MA, Technical Report 16 (September 1971).*

[2] *H.H. Caspers and H. E. Rast, J. Luminescence, 10 (1975), 347.*

**In calculating the multiplet-to-multiplet intensities by using the Judd-Ofelt theory, the agreement with experiment is generally poorer for Pr^{3+} than for the other rare-earth ions. See Selected Bibliography--Multiplet-to-Multiplet Intensities.*

†Earlier line-to-line intensity calculations were made by adjusting the odd-k B_{kq} to fit experimental intensities. Such an approach cannot predict line intensities for arbitrary rare-earth ions or host crystals. Individual line intensities for various rare-earth ions have been calculated by others. See Selected Bibliography--Line Intensities for Rare-Earth Ions, Multiplet-to-Multiplet Intensities for Pr^{3+} Ion, and Multiplet-to-Multiplet Intensities for Nd^{3+} Ion.

Energy levels of other rare-earth ions in YLF have been reported.[3,4,*] The calculated energy levels of Nd^{3+}, for example, were in good agreement with experimental values when only the ground term was considered. However, the model was not as successful when the higher multiplets were included. It was suggested by Nick Karayianis (Harry Diamond Laboratories) that this might be due to interconfiguration mixing, which had not been considered in the calculation. A comparison of calculated and experimental energy levels for Pr^{3+} in YLF is of interest since Pr^{3+} is adjacent to Nd^{3+} in the lanthanide series and since interconfiguration mixing is expected to be even more important[5,6] for Pr^{3+}.

Interest in the Pr^{3+} ion for laser applications has been heightened recently due to the 479-nm laser transition observed[7] in Pr^{3+}:YLF. That study showed that the blue-green laser transition in Pr^{3+}:YLF terminates on the lowest level in the ground state multiplet, indicating three-level laser operation. Since four-level laser action[8] is necessary to achieve high efficiency and low threshold, other hosts[9] are desired where the laser transition terminates on an upper level of the ground multiplet. Numerous experimental studies can be obviated if the energy levels and the transition probabilities for the Pr^{3+} ion in any potential host can be reliably predicted. The adequacy of current theory for reliable prediction has not yet been assessed for Pr^{3+} in any host. The comparison between theory and experiment in this work for

---

[3] *N. Karayianis, D. E. Wortman, and H. P. Jenssen, J. Phys. Chem. Solids, 37 (1976), 675.*

[4] *H. P. Jenssen, A. Linz, R. P. Leavitt, C. A. Morrison, and D. E. Wortman, Phys. Rev. B, 11 (1975), 92.*

[5] *W. Heaps, L. R. Elias, and W. M. Yen, Phys. Rev. B, 13 (1975), 94.*

[6] *K. Rajnak and B. G. Wybourne, J. Chem. Phys., 41 (1964), 565.*

[7] *L. Esterowitz, R. Allen, M. Kruer, F. Bartoli, L. S. Goldberg, H. P. Jenssen, A. Linz, and V. O. Nicolai, J. Appl. Phys., 48 (1977),.650.*

[8] *E. P. Chicklis, C. S. Naiman, R. C. Folweiler, D. R. Gabbe, H. P. Jenssen, and A. Linz, Appl. Phys. Lett., 19 (1971), 119.*

[9] *M. J. Weber in Handbook of Lasers, R. J. Presseley, ed., The Chemical Rubber Co., Cleveland, OH (1971).*

**See Selected Bibliography--Energy Levels of Rare-Earth Ions in YLF.*

Pr^{3+}:YLF provides a useful test of the predictive capability of current crystal field theory.

2. THEORY

2.1 Energy Level Calculations

Two different methods[3,4] for making crystal field calculations for lanthanide ions in host crystals were used here to calculate energy levels and transition probabilities for Pr^{3+} in YLF. Then the experimental results were compared to determine which method describes the measurements more accurately. In method 1, free-ion wave functions were calculated[3] by diagonalizing in a Russell-Saunders basis of J states a Hamiltonian containing the Coulomb, spin-orbit, L^2, $G(G_2)$, and $G(R_7)$ interactions.[10] The free-ion parameters chosen were those obtained by Carnall, Fields, and Rajnak[11] for Pr^{3+} in aqueous solution:

Coulomb parameters: $E^1 = 4548.2$

$E^2 = 21.937$

$E^3 = 466.73$

Spin-orbit parameter: $\zeta = 740.8$

---

[3] *N. Karayianis, D. E. Wortman, and H. P. Jenssen, J. Phys. Chem. Solids, 37 (1976), 675.*

[4] *H. P. Jenssen, A. Linz, R. P. Leavitt, C. A. Morrison, and D. E. Wortman, Phys. Rev. B, 11 (1975), 92.*

[10] *B. G. Wybourne, Spectroscopic Properties of Rare Earths, John Wiley and Sons, Inc., New York (1965).*

[11] *W. T. Carnall, P. R. Fields, and K. J. Rajnak, J. Chem. Phys., 49 (1968), 4424.*

Configuration-interaction parameters: $\alpha = 21.255$

$\beta = -799.94$

$\gamma = 1342.9$

(all in units cm^{-1}). Values of the Slater parameters[10] correspond to those E^i values (in units cm^{-1}):

$F_2 = 305.220$

$F_4 = 46.2767$

$F_6 = 4.43481$

Using this set of free-ion parameters, we calculated reduced matrix elements of U^2, U^4, and U^6 among all of the intermediate coupled wave functions representing the multiplets of the electronic ground configuration of the free ion. A separate program then selected the reduced matrix elements between the free-ion multiplets in a truncated basis (all 13 multiplets for Pr^{3+}), set up the crystal spaces for the given crystal field symmetry (S_4 for YLF), and diagonalized in that space of multiplets the crystal field Hamiltonian given by the expansion

$$H_3 = \sum_{i,k,q} B_{kq}^{+} C_{kq} (i) \quad , \tag{1}$$

where C_{kq} is a spherical tensor of rank k and projection q, and the B_{kq} are the crystal field parameters that describe the effect of the crystal on the free-ion energy levels. The i sum is over the electrons of the $4f^2$ configuration. The S_4 point-group symmetry at the Y^{3+} sites

[10] *B. G. Wybourne, Spectroscopic Properties of Rare Earths, John Wiley and Sons, Inc., New York (1965).*

in the crystal lattice limits the even-k parameters that can be nonzero to B_{20}, B_{40}, B_{60}, B_{44}, and B_{64}.* Although B_{44} and B_{64} can both be complex, one may choose a coordinate system in which B_{44} is real and positive.

In making the above calculations, the centroids associated with the free-ion multiplets were introduced as parameters and were not chosen as the free-ion energies resulting from diagonalizing the free-ion Hamiltonian. In this way, the centroids were freely varied so that, with the full diagonalization of the crystal field Hamiltonian, a more exact fitting to experimental crystal energies was possible. The resultant centroids obtained in this manner reflect what "free-ion" centroids of the rare-earth ion would be observed in the crystal if the even-k components of the static crystal field were "turned off."

In method 2, we simultaneously diagonalized the free-ion and crystal field Hamiltonian in a basis of Russell-Saunders states spanning the entire $4f^2$ electronic configuration. This method had been used[12] in the crystal field analysis of the rare-earth ions in $LaCl_3$. The Hamiltonian used had been[4]

$$H = \sum_i H_i \quad , \tag{2}$$

where, in the notation of Judd[13], H_1 is the Coulomb interaction between the electrons, H_2 is the spin-orbit interaction, H_3 is the crystal field interaction, H_6 is the spin-spin interaction, H_8 is the spin-other-orbit interaction, H_9 is the orbit-orbit interaction, and H_{10} is an effective Hamiltonian representing configuration interaction as given by Rajnak

[4] *H. P. Jenssen, A. Linz, R. P. Leavitt, C. A. Morrison, and D. E. Wortman, Phys. Rev. B, 11 (1975), 92.*

[12] *J. S. Margolis, J. Chem. Phys., 35 (1961), 1367.*

[13] *B. R. Judd, Operator Techniques in Atomic Spectroscopy, McGraw-Hill Book Co., New York (1963).*

**The nonvanishing oddfold parameters in S_4 are B_{32}, B_{52}, B_{72}, and B_{76}.*

and Wybourne.[14] The Pr^{3+} free ion can be described by the Hamiltonian of equation (2) excluding the crystal field interaction H_3, which is given by equation (1). This method has been used with a number of additional interactions to obtain a successful description of most of the rare-earth ion spectra in $LaCl_3$ and LaF_3 (with certain approximations).*

2.2 Intensity Calculations

Intensity calculations were performed by using the Judd-Ofelt[15,16] theory of induced electric dipole transitions. In a spherical basis, the α-component of the induced electric dipole operator is given by[16]

$$p_\alpha = -2 \sum_{\ell k t} \sqrt{\frac{7(2\ell + 1)}{3}} \, (2t + 1) W(k\ell 33; t\ell) R_k(\ell)$$

$$\times \langle \ell(0) 1(0) | 3(0) \rangle \langle 3(0) k(0) | \ell(0) \rangle \left\{ A^{(k)} U^{(t)} \right\}^{(1)}_{\alpha}, \qquad (3)$$

where

$$R_k(\ell) = \sum_n \int R(4f) R(n\ell) r^k \, dr \int R(4f) R(n\ell) r \, dr / \Delta E_{n\ell} \, . \qquad (4)$$

In equation (3), the sum on ℓ covers $\ell = 2$ and 4; the k sum is over k = 1, 3, 5, and 7; and the t sum is over t = 2, 4, and 6. The quantities $\langle j_1(m_1) j_2(m_2) \mid J(M) \rangle$ are Clebsch-Gordon coefficients, $W(k\ell 33;t)$ is a

[14] *K. Rajnak and B. G. Wybourne, Phys. Rev., 132 (1963), 280.*
[15] *B. R. Judd, Phys. Rev., 127 (1962), 750.*
[16] *G. S. Ofelt, J. Chem. Phys., 37 (1962), 511.*
**See Selected Bibliography--Energy Level Structure.*

Racah coefficient, and $A^{(k)}$ is a tensor whose components A_{kq} represent a spherical decomposition of the odd parity part of the crystalline electric field near the rare-earth ion. The quantity $\{A^{(k)}U^{(t)}\}^{(1)}_{\alpha}$ represents the coupling of the tensors $A^{(k)}$ and $U^{(t)}$ to form a tensor of rank 1 and projection α via a Clebsch-Gordon coefficient. In equation (4), $\Delta E_{n\ell}$ is the difference in energy between the configuration $4f^{x-1}n\ell$ (or $nd^9 4f^{x+1}$) and the ground configuration $4fx$ ($x = 2$ for Pr^{3+}). The quantities $R(n\ell)$ are radial wave functions for state $(n\ell)$. For d electrons ($\ell = 2$), the n sum runs over the configurations $3d^9 4f^{x+1}$ and $4d^9 4f^{x+1}$, as well as $4f^{x-1}nd$, $n \geq 5$. For g electrons, the configurations $4f^{x-1}ng$, $n \geq 5$, are considered.

The line strength of a transition is defined as [17]

$$S_{fi} = \sum_{f,i} |\langle f|\vec{p}|i\rangle|^2 \tag{5}$$

where the sums over f,i are over the individual components of the levels f and i.

The integrated absorption coefficient is given by

$$\int \alpha(\nu)\,d\nu = \left(\frac{e^2}{\hbar c}\right)\frac{4\pi^2 c_o \nu_o \chi}{g_i} \sum_{f,i} |\langle f|\vec{\varepsilon}\cdot\vec{p}|i\rangle|^2 \tag{6}$$

where c_o is the concentration of absorbers in ions/cm^3, ν_o is the center frequency of the transition, $\chi = n(n^2 + 2)^2/9$, where n is the index of refraction, g_i is the degeneracy of the initial state, and $\vec{\varepsilon}$ is a unit vector in the direction of polarization of the incoming wave. The integrated absorption coefficient is related to the line strength. For π polarized lines, we have

[17] *E. U. Condon and G. H. Shortley, The Theory of Atomic Spectra, Cambridge University Press, Cambridge, U.K. (1959).*

$$\int \alpha(\nu)\, d\nu = \left(\frac{e^2}{\hbar c}\right) \frac{4\pi^2 c_o \nu_o \chi}{g_i} \; S_{fi} \quad , \tag{7a}$$

and, for polarized lines,

$$\int \alpha(\nu)\, d\nu = \left(\frac{e^2}{\hbar c}\right) \frac{2\pi^2 c_o \nu_o \chi}{g_i} \; S_{fi} \quad . \tag{7b}$$

The factor of 2 difference between equations (7a) and (7b) is due to the different angular distribution of the radiation for these polarizations. For a given ion, the probability per unit time of spontaneous emission of a photon in a direction $\hat{k}$ with polarization $\vec{\epsilon}$ is given by

$$dP_{fi} = \frac{\nu_o^3 e^2 \chi}{(2\pi)^4 g_i c^3 \hbar} \sum_{f,i} |\langle f|\vec{\epsilon}\cdot\vec{p}|i\rangle|^2 \, d\Omega_{\hat{k}} \tag{8}$$

and is proportional to ν_o^2 times the integrated absorption coefficient, with the same coefficient of proportionality for all transitions.

We have evaluated the line strengths for Pr^{3+}:YLF using the Judd-Ofelt induced dipole operator. The quantities $R_k(\ell)$ have been evaluated by using two assumptions:

a. $R_k(d)$ is dominated by the 4f-5d transition. The configuration $4f^{x-1}5d$ is separated from $4f^x$ by ΔE_{5d}. We assume that $\langle 4f|r^k|5d\rangle = (\tau')^{-k}\langle 4f|r^k|5d\rangle_{HF}$ with $\tau' = 0.81$, to compute the $R_k(d)$ using Hartree-Fock (HF) wave functions.[18]

[18] *P. Grossgut, Doctoral Dissertation, Texas Christian University (1971); University Microfilms, Ann Arbor, MI, No. 72-7621.*

b. $R_k(g)$ is evaluated by assuming that all $4f^{x-1}ng$ configurations are approximately degenerate at a separation ΔE_g from $4f^x$ and by using the closure property of the set R(ng). We assume that $\langle 4f|r^k|4f\rangle = \tau^{-k}\langle 4f|r^k|4f\rangle_{HF}$ with $\tau = 0.76$, to compute the $R_k(g)$ by using HF wave functions.[19] Using[20] $\Delta E_{5d} = 61{,}200\ cm^{-1}$ and $\Delta E_g = 238{,}400\ cm^{-1}$, we have arrived at the following set of $R_k(\ell)$ for Pr^{3+}:

$$R_1(d) = 3.324 \qquad R_1(g) = 2.210$$

$$R_3(d) = 6.839 \qquad R_3(g) = 2.786$$

$$R_5(d) = 22.98 \qquad R_5(g) = 7.538$$

$$R_7(g) = 36.35$$

The units of $R_k(\ell)$ are $10^{-6}\ (\mathring{A})^{k+1}/cm^{-1}$. This is the first time that these quantities have been calculated from first principles.

The crystal field components, A_{kq}, have been computed by using an effective point charge model[21] with a charge of +3 on the yttrium ion, +1 on the lithium ion, and -1 on the fluorine ion. These give the following values for the odd-k A_{kq} (rotated to a frame where A_{44} is real and positive):

---

[19] *A. J. Freeman and R. E. Watson, Phys. Rev., 127 (1962), 2058.*

[20] *Clyde A. Morrison, Nick Karayianis, and Donald E. Wortman, Rare-Earth Ion-Host Lattice Interactions 4. Predicting Spectra and Intensities of Lanthanides in Crystals, Harry Diamond Laboratories TR-1816 (June 1977).*

[21] *D. E. Wortman, N. Karayianis, and C. A. Morrison, Rare-Earth Ion-Host Lattice Interactions 6. Lanthanides in $LiYF_4$, Harry Diamond Laboratories TR-1770 (August 1976).*

$$A_{32} = 657 - 667i$$

$$A_{52} = -2671 - 59i$$

$$A_{72} = 7 + 14i$$

$$A_{76} = 254 + 45i$$

The units of A_{kq} are $cm^{-1}/(\mathring{A})^k$.

Electric dipole transition probabilities were calculated by using the full intermediate coupling J-mixed wave functions (method 1).

2.3 Symmetry Considerations

The eigenstates obtained in the above calculations transform[22] according to one of four irreducible representations (Γ_1, Γ_2, Γ_3, and Γ_4) of the S_4 point group. The levels characterized by wave functions transforming as Γ_3 and Γ_4 are degenerate and are designated $\Gamma_{3,4}$. The space is 91 dimensional and separates into a 25 × 25, a 24 × 24, and two 21 × 21 matrices. The first two and one of the last need to be diagonalized to determine, respectively, the energy levels for Γ_1, Γ_2, and $\Gamma_{3,4}$.

The experimental energy levels are classified by analyzing the polarization data. According to the transformation properties of the electric dipole operator, identical axial and parallelly (σ-) polarized spectra (within a multiplicative factor) require the use of electric dipole selection rules. Identical axial and perpendicularly (π-) polarized spectra require the use of magnetic dipole selection rules. A

---

[22] *G. F. Koster, J. O. Dimmock, R. G. Wheeler, and H. Statz, Properties of the Thirty-Two Point Groups, MIT Press, Cambridge, MA (1963).*

comparison of measured σ, π, and axial spectra for Pr^{3+}:YLF indicates that electric dipole transitions predominate.

In examining the spectra, we also considered selection rules[22] for D_{2d} point-group symmetry (S_4 is a subgroup of D_2) to explain many of the low-intensity lines. If the Pr^{3+} ion were in a site of D_{2d} symmetry, certain transitions would be forbidden, as shown in table I. If, however, the local site symmetry were perturbed by a lower symmetry environment, such as S_4, some of the forbiddenness would be lifted. In addition, in the energy-level calculations, the imaginary component of B_{64} (Im B_{64}) is a certain measure of the difference between D_{2d} and S_4. The odd-k B_{kq}, however, enter the intensity calculations, and even if Im $B_{64} = 0$, the imaginary B_{kq} for odd-k are not necessarily small in S_4; they are 0 in D_{2d}.* Since we have considered both S_4 and D_{2d}, we have listed the corresponding identifications of the S_4 levels in D_{2d} notation in table II. The full rotation-group compatibility tables for S_4 and D_{2d} are given in table III.

---

[22] *G. F. Koster, J. O. Dimmock, R. G. Wheeler, and H. Statz, Properties of the Thirty-Two Point Groups, Massachusetts Institute of Technology, Cambridge, MA (1963).*

**The transition to D_{2d} symmetry may be performed in either of two ways: (1) by making B_{44} and B_{64} real and making all the odd-k B_{kq} real or (2) by making B_{44} and B_{64} real and making all the odd-k B_{kq} pure imaginary. The second way is usually chosen; it is related to the first by a rotation of 45 deg about the fourfold symmetry axis. In particular, the B_{kq} in the second way may be obtained from those in the first by changing the sign of B_{44} and B_{64}; multiplying B_{32}, B_{52}, and B_{72} by i; and multiplying B_{76} by $(-i)$. We have chosen the first way since it agrees with our convention of choosing $B_{44} > 0$.*

TABLE I. ELECTRIC DIPOLE SELECTION RULES IN S_4 AND D_{2d}

S_4	Γ_1	Γ_2	Γ_3	Γ_4
Γ_1	-	π	σ	σ
Γ_2	π	-	σ	σ
Γ_3	σ	σ	-	π
Γ_4	σ	σ	π	-

D_{2d}	Γ_1	Γ_2	Γ_3	Γ_4	Γ_5
Γ_1	-	-	-	π	σ
Γ_2	-	-	π	-	σ
Γ_3	-	π	-	-	σ
Γ_4	π	-	-	-	σ
Γ_5	σ	σ	σ	σ	π

Note: This notation corresponds to that of G. F. Koster et al, Properties of the Thirty-Two Point Groups, Massachusetts Institute of Technology, Cambridge, MA (1963). A coordinate system rotated by $\pi/4$ about the z-axis gave correct, but different selection rules in H. P. Jenssen et al, Phys. Rev. B, 11 (1975), 92.

TABLE II. IDENTIFICATIONS OF IRREDUCIBLE REPRESENTATIONS OF D_{2d} POINT GROUP IN S_4 NOTATION

S_4	D_{2d}
Γ_1	Γ_1
	Γ_2
Γ_2	Γ_3
	Γ_4
$\Gamma_{3,4}$	Γ_5

TABLE III. FULL ROTATION-GROUP COMPATIBILITY TABLES FOR S_4 and D_{2d}

	S_4	D_{2d}
D_0^+	Γ_1	Γ_1
D_1^+	$\Gamma_1 + (\Gamma_3 + \Gamma_4)$	$\Gamma_2 + (\Gamma_5)$
D_2^+	$\Gamma_1 + 2[\Gamma_2] + (\Gamma_3 + \Gamma_4)$	$\Gamma_1 + [\Gamma_3 + \Gamma_4] + (\Gamma_5)$
D_3^+	$\Gamma_1 + 2[\Gamma_2] + 2(\Gamma_3 + \Gamma_4)$	$\Gamma_2 + [\Gamma_3 + \Gamma_4] + 2(\Gamma_5)$
D_4^+	$3\Gamma_1 + 2[\Gamma_2] + 2(\Gamma_3 + \Gamma_4)$	$2\Gamma_1 + \Gamma_2 + [\Gamma_3 + \Gamma_4] + 2(\Gamma_5)$
D_5^+	$3\Gamma_1 + 2[\Gamma_2] + 3(\Gamma_3 + \Gamma_4)$	$\Gamma_1 + 2\Gamma_2 + [\Gamma_3 + \Gamma_4] + 3(\Gamma_5)$
D_6^+	$3\Gamma_1 + 4[\Gamma_2] + 3(\Gamma_3 + \Gamma_4)$	$2\Gamma_1 + \Gamma_2 + 2[\Gamma_3 + \Gamma_4] + 3(\Gamma_5)$

Note: The irreducible representations in parentheses (or brackets) in S_4 relate to those in parentheses (or brackets) in D_{2d}.

Source: G. F. Koster et al, Properties of the Thirty-Two Point Groups, Massachusetts Institute of Technology, Cambridge, MA (1963).

3. EXPERIMENTAL PROCEDURE

Fluorescence and absorption measurements were obtained by using a high-resolution 0.85-m Spex double monochromator for emission lines between 31,600 and 90,650 cm^{-1}. Lower energy fluorescence lines were obtained by using a 1-m McPherson spectrometer with interchangeable gratings. In the Spex double monochromator, a pair of 1200-groove/mm gratings yields a maximum resolution better than 0.2 cm^{-1}. The McPherson spectrometer was operated with 600 grooves/mm at a resolution better than 1 cm^{-1}. Above 12,000 cm^{-1}, signals were detected by an RCA C31034A gallium arsenide (GaAs) photomultiplier tube cooled to -30 C and photon counting electronics. Below 12,000 cm^{-1}, signals were detected by an RCA C30811 silicon (Si) avalanche photodiode, the optical source was chopped, and the detector signal was measured by a PARC 124 lock-in amplifier with a PARC 116 plug-in preamplifier.

The samples used in this study were high optical quality YLF crystals grown at the Massachusetts Institute of Technology by using a top-seeded-solution technique. The crystals were grown in a purified argon atmosphere from a *nonstoichiometric* melt containing YF_3 and a slight excess of LiF. The Pr^{3+} ions enter substitutionally for Y^{3+}. The concentration of Pr^{3+} in the crystals studied is nominally 0.2 at.%. Samples were cut with two faces perpendicular to the c-axis of the crystals, and all faces were optically polished.

Crystal samples were mounted in an Air Products closed-cycle refrigerator capable of operating between 8 and 300 K. The temperature of the sample was regulated to within 0.1 K by using a GaAs temperature sensing diode and a PARC 152 temperature controller.

Laser excited fluorescence was measured; a focused laser beam was propagated perpendicularly to both the axis of observation and the c-axis of the Pr^{3+}:YLF crystal. The 4765-Å line of a cw argon laser, polarized parallel to the c-axis (π), was used to pump the crystal for $^3P_0$ fluorescence. For $^1D_2$ fluorescence measurements, an argon-laser-pumped dye laser was used to pump the $^1D_2$ level directly. The focused dye laser beam was polarized perpendicularly to the c-axis (σ) and was tuned slightly above the 17,083-cm^{-1} σ absorption of the Pr^{3+} ion to achieve relatively uniform absorption and to avoid heating the sample. At both laser wavelengths, the laser power incident on the crystal was several hundred milliwatts. The greater sensitivity obtained by laser excitation permitted the observation of weak emission lines not found by using incoherent sources.[2]

Absorption was measured by illuminating the crystal perpendicularly to the c-axis with parallel light from a tungsten lamp. In both absorption and fluorescence experiments, light from the sample was collected by a double lens system that produced parallel light between the lenses. Polarization was selected by a Glan-Thompson polarizer. To

[2] *H. H. Caspers and H. E. Rast, J. Luminescence, 10 (1975), 347.*

compensate for the polarization sensitivity of the spectrometers, a $\lambda/2$ achromatic Fresnel rhomb retarder with a 25-mm clear aperture was placed in the parallel light between the lenses. This device rotated the polarization of the optical signals by an arbitrary angle so that both π- and σ-polarized light entered the spectrometers with the same polarization. The wavelength readouts of the spectrometers were calibrated by using the first and second orders of mercury emission lines and of various lines of argon and helium-neon (He-Ne) lasers.

4. EXPERIMENTAL RESULTS

Results of fluorescence and absorption measurements are summarized in tables IV to XII for the $^3H_4$, $^3H_5$, $^3H_6$, $^3F_2$, $^3F_3$, $^3F_4$, $^1G_4$, $^1D_2$, $^3P_0$, $^3P_1$, and $^3P_2$ states. The tables present the line frequency in a vacuum, the polarization and relative intensity, S_4 symmetry assignment, and the derived energy levels for each multiplet. The spectra reported were obtained at 10, 30, and 80 K. The temperatures listed in the tables refer to the lowest of these three temperatures at which the transition was observed. The intensities reported for absorption refer to the integral over frequency of the absorptance $A = -\log_{10} (I_t/I_i)$, where I_t and I_i are the transmitted and incident intensities, respectively. Only relative intensities are given for both absorption and fluorescence, the strongest line for each multiplet being normalized to 1000. Relative intensities between multiplets or between $^3P_0$ and $^1D_2$ fluorescence are not presented. Identifications of energy levels of Pr^{3+} in YLF are consistent with electric dipole selection rules. Magnetic dipole transitions also were found, but these were generally less intense than the electric dipole transitions.

The $^3P_0$ and $^1D_2$ absorption data (table IV) basically agree with those of Jenssen[1] and of Caspers and Rast,[2] although our line positions agree more closely with those of Caspers and Rast.[2] The absorption spectra from the $^3H_4$ multiplet to the singlet $^3P_0$ Γ_1 level contain only one π-polarized line at 20,860 cm^{-1} at low temperatures. Assuming electric dipole transitions and S_4 site symmetry, these indicate that the lowest level in the $^3H_4$ multiplet is Γ_2. At higher temperatures, a σ-polarized absorption line is observed at 20,781 cm^{-1}, indicating that there is a $\Gamma_{3,4}$ level 79 cm^{-1} above the ground state in the $^3H_4$ multiplet.

TABLE IV. ABSORPTION OF $^3P_0$ AND $^1D_2$ LEVELS IN Pr^{3+}: $LiYF_4$ AT 10, 30, AND 80 K

		$^3H_4 \rightarrow {}^3P_0$			
Line	Line frequency in vacuum (cm^{-1})	Polarization* and relative intensity	Temp (K)	S_4 symmetry assignment	Derived energy level for $^3P_0$ (cm^{-1})
1	20,860	π	10	$\Gamma_2 \rightarrow \Gamma_1$	20,860
2	20,781	σ	30	$\Gamma_{3,4} \rightarrow \Gamma_1$	20,860
		$^3H_4 \rightarrow {}^1D_2$			
Line	Line frequency in vacuum (cm^{-1})	Polarization* and relative intensity	Temp (K)	S_4 symmetry assignment	Derived energy level for $^1D_2$ (cm^{-1})
1	16,661	3σ	30	$\Gamma_{3,4} \rightarrow \Gamma_2$	16,740
2	16,731	8σ	30	$\Gamma_{3,4} \rightarrow \Gamma_1$	16,810
3	16,810	1000π	10	$\Gamma_2 \rightarrow \Gamma_1$	16,810
4	17,004†	π	80	$\Gamma_{3,4} \rightarrow \Gamma_{3,4}$	17,083†
5	17,083†	797σ†	10	$\Gamma_2 \rightarrow \Gamma_{3,4}$	17,083†
6	17,327	σ	80	$\Gamma_{3,4} \rightarrow \Gamma_2$	17,406

*π = polarized with electric vector parallel to c-axis; σ = polarized perpendicularly to c-axis.

†Broad line ($\sim$ 100 cm^{-1}) with structure superimposed.

[1] H.P. Jenssen, Phonon Assisted Laser Transitions and Energy Transfer in Rare Earth Laser Crystals, Massachusetts Institute of Technology Crystal Physics Laboratory, Cambridge, MA, Technical Report 16 (September 1971).

[2] H. H. Caspers and H. E. Rast, J. Luminescence, 10 (1975), 347.

In S_4 symmetry, the $^1D_2$ multiplet splits into one Γ_1 level, two Γ_2 levels, and one $\Gamma_{3,4}$ level. According to electric dipole selection rules for S_4 symmetry, the low temperature $^1D_2$ absorption should contain one π and one σ line. Table IV shows that one π line and one σ line are observed at 16,810 cm^{-1} (line 3) and 17,083 cm^{-1} (line 5), respectively. At higher temperatures, absorption from the 79 cm^{-1} $\Gamma_{3,4}$ level to $^1D_2$ should contain three σ lines and one π line. As shown in table IV, all four lines were observed although lines 1 and 2 were observed at 30 K, but lines 4 and 6 were not observed below 80 K. These absorption measurements permit a complete identification of the $^1D_2$ energy levels. The lowest $^1D_2$ level at 16,740 cm^{-1} is Γ_2 with a Γ_1 level 70 cm^{-1} above it at 16,810 cm^{-1}. All $^1D_2$ fluorescence reported in this work originates at these two levels. The remaining $^1D_2$ levels consist of a $\Gamma_{3,4}$ level at 17,083 cm^{-1} and a Γ_2 level at 17,406 cm^{-1}.

The energy levels of the $^3H_4$ multiplet were established from $^3P_0$ and $^1D_2$ fluorescence measurements in table V. In S_4 symmetry, the $^3H_4$ multiplet splits into three Γ_1, two Γ_2, and two $\Gamma_{3,4}$ levels. From the electric dipole selection rules for S_4 symmetry the $^3P_0$ Γ_1 fluorescence spectra are expected to contain two π-polarized lines corresponding to $\Gamma_1 \rightarrow \Gamma_2$ transitions and two σ-polarized lines corresponding to $\Gamma_1 \rightarrow \Gamma_{3,4}$ transitions. As shown in table V, two σ lines and only one π line were observed. The missing π line corresponds to one of the two Γ_2 levels in the $^3H_4$ multiplet.

Electric dipole transitions from the lower $^1D_2$ Γ_2 energy level at 16,740 cm^{-1} to the Γ_1 levels in $^3H_4$ are expected to be π polarized, whereas transitions to the $\Gamma_{3,4}$ levels are expected to be σ polarized. In the low temperature fluorescence measurements, the two expected σ lines were observed and are listed as lines 4a and 7 in table V. Only one π line (line 5) was observed. Line 5 may represent two unresolved Γ_1 levels that are predicted theoretically to be extremely close in energy (table XII). At higher temperatures, transitions are

TABLE V. OBSERVED $^3P_0 \rightarrow {}^3H_4$ AND $^1D_2 \rightarrow {}^3H_4$ FLUORESCENCE FOR Pr^{3+}: $LiYF_4$

$^1D_2 \rightarrow {}^3H_4$

Line	Line frequency in vacuum (cm^{-1})	Polarization* and relative intensity	Temp (K)	S_4 symmetry assignment	Derived energy level for $^3H_4$ (cm^{-1})
1	16,810	π	30	$\Gamma_1 \rightarrow \Gamma_2$	0
2	16,740	5σ	10	$\Gamma_2 \rightarrow \Gamma_2$†	0
3	16,731	σ	30	$\Gamma_1 \rightarrow \Gamma_{3,4}$	79
4a	16,661	1000σ	10	$\Gamma_2 \rightarrow \Gamma_{3,4}$	79
4b	16,661	11π‡	10	$\Gamma_2 \rightarrow \Gamma_{3,4}$†	79
5	16,520	102π	10	$\Gamma_2 \rightarrow \Gamma_1$	220§
6	16,314	σ	80	$\Gamma_1 \rightarrow \Gamma_{3,4}$	496
7	16,244	891σ	10	$\Gamma_2 \rightarrow \Gamma_{3,4}$	496

$^3P_0 \rightarrow {}^3H_4$ (10 K)

Line	Line frequency in vacuum (cm^{-1})	Polarization* and relative intensity	S_4 symmetry assignment	Derived energy level for $^3H_4$ (cm^{-1})
1	20,860	1000π	$\Gamma_1 \rightarrow \Gamma_2$	0
2	20,781	249σ	$\Gamma_1 \rightarrow \Gamma_{3,4}$	79
3	20,364	94σ	$\Gamma_1 \rightarrow \Gamma_{3,4}$	496

*π = polarized parallel to c-axis; σ = polarized perpendicularly to c-axis.

†Tentatively identified as magnetic dipole transitions.

‡ Intensity is uncertain because of vibronic structure in spectrum.

§May represent two Γ_1 levels that are predicted theoretically to be extremely close (see table XII).

expected from the $^1D_2$ Γ_1 level at 16,810 cm^{-1} to the two Γ_2 (π) and two $\Gamma_{3,4}$ (σ) levels. As shown in table V, the two σ lines were observed (lines 3 and 6), but only one π line (line 1) was observed. The levels established by these three lines agree well with those determined from the $^3P_0$ fluorescence spectra. The two remaining lines in the $^1D_2$ fluorescence (lines 2 and 4b) are tentatively identified as magnetic dipole transitions.

The $^3H_5$ energy levels were established from the fluorescence data listed in table VI. In S_4 symmetry, the $^3H_5$ multiplet splits into three Γ_1, two Γ_2, and three $\Gamma_{3,4}$ levels. For electric dipole transitions, two π-polarized lines and three σ-polarized lines are expected in $^3P_0$ fluorescence. As shown in table VI, the two π lines (lines 2 and 4) and the three σ lines (lines 1, 3, and 5) were all observed. Because of vibronic structure extending over a region 140 cm^{-1} wide, the energy of line 5 is not well defined.

According to electric dipole selection rules, fluorescence from the $^1D_2$ Γ_2 level at 16,740 cm^{-1} is expected to contain three π lines corresponding to Γ_1 levels in $^3H_5$ and three σ lines corresponding to $\Gamma_{3,4}$ levels. As shown in table VI, three π lines (lines 1, 3, and 5) and three π lines (lines 2, 4, and 6) were observed. Lines 5 and 6 are very broad and have vibronic structure, and their energies are not well defined. The $^3P_0$ and $^1D_2$ fluorescence measurements allow us to account for all eight $^3H_5$ energy levels, although the energies of one Γ_1 and one $\Gamma_{3,4}$ level are not well established.

The energy levels of the $^3H_6$ multiplet were established from $^3P_0$ and $^1D_2$ fluorescence measurements in table VII. The $^3H_6$ manifold splits into three Γ_1, four Γ_2, and three $\Gamma_{3,4}$ levels. Electric dipole transitions from the $^3P_0$ Γ_1 level to the four Γ_2 levels are expected to appear in π polarization and those to the three $\Gamma_{3,4}$ levels in σ polarization. As shown in table VII, all three σ lines are observed, but only three of the four π lines have been found.

TABLE VI. OBSERVED $^3P_0 \rightarrow {}^3H_5$ AND $^1D_2 \rightarrow {}^3H_5$ FLUORESCENCE FOR Pr^{3+}: $LiYF_4$

$^3P_0 \rightarrow {}^3H_5$

Line	Line frequency in vacuum (cm^{-1})	Polarization* and relative intensity	Temp (K)	S_4 symmetry assignment	Derived energy level for $^3H_5$ (cm^{-1})
1	18,588	120σ	10	$\Gamma_1 \rightarrow \Gamma_{3,4}$	2272
2	18,580	20π	10	$\Gamma_1 \rightarrow \Gamma_2$	2280
3	18,519	81σ	10	$\Gamma_1 \rightarrow \Gamma_{3,4}$	2341
4	18,311	950π	10	$\Gamma_1 \rightarrow \Gamma_2$	2549
5	18,180 to 18,320†	1000σ†	10	$\Gamma_1 \rightarrow \Gamma_{3,4}$	2540 to 2680†

$^1D_2 \rightarrow {}^3H_5$

Line	Line frequency in vacuum (cm^{-1})	Polarization* and relative intensity	Temp (K)	S_4 symmetry assignment	Derived energy level for $^3H_5$ (cm^{-1})
1	14,487	200π	10	$\Gamma_2 \rightarrow \Gamma_1$	2253
2	14,468	1000σ	10	$\Gamma_2 \rightarrow \Gamma_{3,4}$	2272
3	14,443	2π	10	$\Gamma_2 \rightarrow \Gamma_1$	2297
4	14,399	55σ	10	$\Gamma_2 \rightarrow \Gamma_{3,4}$	2341
5	14,075 to 14,205†	1000π†	10	$\Gamma_2 \rightarrow \Gamma_1$	2535 to 2665†
6	14,060 to 14,200†	280σ†	10	$\Gamma_2 \rightarrow \Gamma_{3,4}$	2540 to 2680†

*π = *polarized parallel to c-axis*; σ = *polarized perpendicularly to c-axis.*

†*Very broad structured band.*

TABLE VII. OBSERVED $^3P_0 \rightarrow {}^3H_6$ AND $^1D_2 \rightarrow {}^3H_6$ FLUORESCENCE FOR Pr^{3+}: $LiYF_4$

$^3P_0 \rightarrow {}^3H_6$

Line	Line frequency in vacuum (cm^{-1})	Polarization* and relative intensity	Temp (K)	S_4 symmetry assignment	Derived energy level for $^3H_6$ (cm^{-1})
1	16,546	>1000π	10	$\Gamma_1 \rightarrow \Gamma_2$	4314
2	16,466	>1000σ	10	$\Gamma_1 \rightarrow \Gamma_{3,4}$	4394
3	16,406	675σ	10	$\Gamma_1 \rightarrow \Gamma_{3,4}$	4454
4	16,303‡	813π†	10	$\Gamma_1 \rightarrow \Gamma_2$	4557‡
5	15,953	198σ	10	$\Gamma_1 \rightarrow \Gamma_{3,4}$	4907
6	15,915	37π	10	$\Gamma_1 \rightarrow \Gamma_2$	4945

$^1D_2 \rightarrow {}^3H_6$

Line	Line frequency in vacuum (cm^{-1})	Polarization* and relative intensity	Temp (K)	S_4 symmetry assignment	Derived energy level for $^3H_6$ (cm^{-1})
1	12,496	83π	30	$\Gamma_1 \rightarrow \Gamma_2$	4314
2	12,426	3σ	10	$\Gamma_2 \rightarrow \Gamma_2$†	4314
3a	12,346	1000σ	10	$\Gamma_2 \rightarrow \Gamma_{3,4}$	4394
3b	12,346	21π	10	$\Gamma_2 \rightarrow \Gamma_{3,4}$†	4394
4	12,286	139σ	10	$\Gamma_2 \rightarrow \Gamma_{3,4}$	4454
5	12,254	284π	10	$\Gamma_2 \rightarrow \Gamma_1$	4486
6	11,833	190σ	10	$\Gamma_2 \rightarrow \Gamma_{3,4}$	4907

*π = polarized parallel to c-axis; σ = polarized perpendicularly to c-axis.

†Tentatively identified as magnetic dipole transitions.

‡Line position and relative intensity are uncertain because of vibronic structure in spectrum.

Electric dipole transitions from the $^1D_2$ Γ_2 level at 16,740 cm^{-1} should include three π and three σ lines. Three σ lines (lines 3a, 4, and 6) were observed, and the $^3H_6$ $\Gamma_{3,4}$ levels obtained agree well with the $^3P_0$ fluorescence results. Only one of the three π lines (line 5) corresponding to the Γ_1 energy levels was observed. At higher temperatures, fluorescence from the $^1D_2$ Γ_1 level also is expected. Table VII shows that one such line (line 1) was observed at 30 K. Two of the observed lines listed in table VII (lines

2 and 3b) are tentatively identified as magnetic dipole transitions. From the $^3P_0$ and $^1D_2$ fluorescence, all but one Γ_1 and two Γ_2 levels have been established.

The $^3F_2$ energy levels were established from fluorescence measurements in table VIII. The $^3F_2$ multiplet splits into one Γ_1, two Γ_2, and one $\Gamma_{3,4}$ levels. Two π-polarized lines and one σ-polarized line are expected in fluorescence from the $^3P_0$ Γ_1 level. Table VIII shows that all three lines are observed.

TABLE VIII. OBSERVED $^3P_0 \rightarrow {}^3F_2$ AND $^1D_2 \rightarrow {}^3F_2$ FLUORESCENCE FOR Pr^{3+}: LiYF$_4$

$^3P_0 \rightarrow {}^3F_2$

Line	Line frequency in vacuum (cm^{-1})	Polarization* and relative intensity	Temp (K)	S_4 symmetry assignment	Derived energy level for $^3F_2$ (cm^{-1})
1	15,659	186π	10	$\Gamma_1 \rightarrow \Gamma_2$	5201
2	15,637	1000σ	10	$\Gamma_1 \rightarrow \Gamma_{3,4}$	5221
3	15,518	366π	10	$\Gamma_1 \rightarrow \Gamma_2$	5342

$^1D_2 \rightarrow {}^3F_2$

Line	Line frequency in vacuum (cm^{-1})	Polarization* and relative intensity	Temp (K)	S_4 symmetry assignment	Derived energy level for $^3F_2$ (cm^{-1})
1	11,609	>1000π	80	$\Gamma_1 \rightarrow \Gamma_2$	5201
2	11,589	732σ	80	$\Gamma_1 \rightarrow \Gamma_{3,4}$	5221
3	11,539	68σ	10	$\Gamma_2 \rightarrow \Gamma_2$†	5201
4a	11,519	1000σ	10	$\Gamma_2 \rightarrow \Gamma_{3,4}$	5221
4b	11,519	100π	10	$\Gamma_2 \rightarrow \Gamma_{3,4}$†	5221

*π = polarized parallel to c-axis; σ = polarized perpendicularly to c-axis.

†Tentatively identified as magnetic dipole transitions.

Electric dipole transitions originating at the $^1D_2$ Γ_2 level are expected to include one π line and one σ line. Line 4a, observed at 10 K in the σ polarization, agrees well with the $^3P_0$ σ transition (line 2). The π transition to the $^3F_2$ Γ_1 level was not observed. Lines 3 and 4b

in the $^1D_2$ fluorescence are tentatively identified as magnetic dipole transitions. At higher temperatures, fluorescence from the $^1D_2$ Γ_1 level is expected to include one σ and two π lines. Table VIII shows that the σ line (line 2) and one of the two π lines (line 1) were observed and found to agree well with lines 1 and 2 of the $^3P_0$ fluorescence. The fluorescence measurements allow us to establish all but the Γ_1 level of the $^3F_2$ multiplet.

All the energy levels of the $^3F_3$ multiplet can be established from the $^3P_0$ and $^1D_2$ fluorescence spectra in table IX. For S_4 symmetry, the $^3F_3$ multiplet splits into one Γ_1, two Γ_2, and two $\Gamma_{3,4}$ energy levels. According to electric dipole selection rules, the $^3P_0$ fluorescence spectra are expected to contain two π-polarized lines corresponding to $\Gamma_1 \rightarrow \Gamma_2$ transitions and two σ-polarized lines corresponding to $\Gamma_1 \rightarrow \Gamma_{3,4}$ transitions. As shown in table IX, the four expected lines are observed.

Electric dipole transitions from the $^1D_2$ Γ_2 level at 16,740 cm^{-1} to the Γ_1 level and two $\Gamma_{3,4}$ levels of $^3F_3$ are expected to be π polarized and σ polarized, respectively. These three transitions have been observed at 10 K and are listed as lines 3a, 5, and 8a in table IX. At higher temperatures, emission from the Γ_1 level of the $^1D_2$ multiplet to the two Γ_2 and two $\Gamma_{3,4}$ levels of $^3F_3$ also is expected. Table IX lists these four lines (lines 1, 2, 6, and 7) and their observed polarizations, which are consistent with electric dipole transitions. This completes the determination of the $^3F_3$ energy levels. Three extra lines (lines 3b, 4, and 8b) also observed in the low temperature $^1D_2$ fluorescence are tentatively identified as magnetic dipole transitions.

The $^3F_4$ energy levels were established from the fluorescence data in table X. The $^3F_4$ multiplet splits into three Γ_1, two Γ_2, and two $\Gamma_{3,4}$ energy levels. From electric dipole selection rules, we expect

two σ-polarized and two π-polarized lines in the $^3P_0$ fluorescence. As shown in table X, both σ lines are observed, but only one of the π lines was found.

TABLE IX. OBSERVED $^3P_0 \rightarrow {}^3F_3$ AND $^1D_2 \rightarrow {}^3F_3$ FLUORESCENCE FOR Pr^{3+}: $LiYF_4$

$^3P_0 \rightarrow {}^3F_3$

Line	Line frequency in vacuum (cm^{-1})	Polarization* and relative intensity	Temp (K)	S_4 symmetry assignment	Derived energy level for $^3F_3$ (cm^{-1})
1	14,379	17σ	10	$\Gamma_1 \rightarrow \Gamma_{3,4}$	6481
2	14,339	1000π	10	$\Gamma_1 \rightarrow \Gamma_2$	6521
3	14,189	2σ	10	$\Gamma_1 \rightarrow \Gamma_{3,4}$	6671
4	14,174	78π	10	$\Gamma_1 \rightarrow \Gamma_2$	6686

$^1D_2 \rightarrow {}^3F_3$

Line	Line frequency in vacuum (cm^{-1})	Polarization* and relative intensity	Temp (K)	S_4 symmetry assignment	Derived energy level for $^3F_3$ (cm^{-1})
1	10,329	4σ	30	$\Gamma_1 \rightarrow \Gamma_{3,4}$	6481
2	10,289	67π	30	$\Gamma_1 \rightarrow \Gamma_2$	6521
3a	10,259	753σ	10	$\Gamma_2 \rightarrow \Gamma_{3,4}$	6481
3b	10,259	13π	10	$\Gamma_2 \rightarrow \Gamma_{3,4}$†	6481
4	10,219	35σ	10	$\Gamma_2 \rightarrow \Gamma_2$†	6521
5	10,154	1000π	10	$\Gamma_2 \rightarrow \Gamma_1$	6586
6	10,139	13σ	30	$\Gamma_1 \rightarrow \Gamma_{3,4}$	6671
7	10,124	π	80	$\Gamma_1 \rightarrow \Gamma_2$	6686
8a	10,069	442σ	10	$\Gamma_2 \rightarrow \Gamma_{3,4}$	6671
8b	10,069	22π	10	$\Gamma_2 \rightarrow \Gamma_{3,4}$†	6671

*π = polarized parallel to c-axis; σ = polarized perpendicularly to c-axis.

†Tentatively identified as magnetic dipole transitions.

TABLE X. OBSERVED $^3P_0 \rightarrow {}^3F_4$ AND $^1D_2 \rightarrow {}^3F_4$ FLUORESCENCE FOR Pr^{3+}: $LiYF_4$

$^3P_0 \rightarrow {}^3F_4$

Line	Line frequency in vacuum (cm^{-1})	Polarization* and relative intensity	Temp (K)	S_4 symmetry assignment	Derived energy level for $^3F_4$ (cm^{-1})
1	13,918	8σ	10	$\Gamma_1 \rightarrow \Gamma_{3,4}$	6942
2	13,877	1000π	10	$\Gamma_1 \rightarrow \Gamma_2$	6983
3	13,718	2σ	10	$\Gamma_1 \rightarrow \Gamma_{3,4}$	7142

$^1D_2 \rightarrow {}^3F_4$

Line	Line frequency in vacuum (cm^{-1})	Polarization* and relative intensity	Temp (K)	S_4 symmetry assignment	Derived energy level for $^3F_4$ (cm^{-1})
1	9868	10σ	30	$\Gamma_1 \rightarrow \Gamma_{3,4}$	6942
2	9827	π†	30	$\Gamma_1 \rightarrow \Gamma_2$	6983
3	9820	148π	10	$\Gamma_2 \rightarrow \Gamma_1$	6920
4	9798	182σ	10	$\Gamma_2 \rightarrow \Gamma_{3,4}$	6942
5	9694	π	80	$\Gamma_1 \rightarrow \Gamma_2$	7116
6	9668	9σ	30	$\Gamma_1 \rightarrow \Gamma_{3,4}$	7142
7	9635	611π	10	$\Gamma_2 \rightarrow \Gamma_1$	7105
8	9598	1000σ	10	$\Gamma_2 \rightarrow \Gamma_{3,4}$	7142
9	9518	371π	10	$\Gamma_2 \rightarrow \Gamma_1$	7220

*π = polarized parallel to c-axis; σ = polarized perpendicularly to c-axis.

†Weak temperature-dependent shoulder.

From the $^1D_2$ Γ_2 level, three π lines and two σ lines are expected for electric dipole transitions. All five transitions were observed at low temperatures (lines 3, 4, 7, 8, and 9). At higher temperatures, fluorescence from the $^1D_2$ Γ_1 level is expected to include two σ-polarized and two π-polarized lines. Table X lists the four observed lines, which include transitions to the same three levels observed in the $^3P_0$ fluorescence and the one Γ_2 level not observed. As shown in the table, $^3F_4$ energy levels determined from both $^3P_0$ and $^1D_2$ fluorescence agree well. These measurements allow us to completely establish all the levels of the $^3F_4$ multiplet.

The energy levels of the $^1G_4$ multiplet were established from $^3P_0$ fluorescence and absorption data in table XI. On the basis of S_4 electric dipole selection rules, the $^3P_0$ fluorescence is expected to contain two π-polarized and two σ-polarized lines. Table XI shows that the two expected π lines were observed (lines 2 and 3), but only one σ line was seen.

TABLE XI. OBSERVED $^3P_0 \rightarrow {}^1G_4$ FLUORESCENCE AND $^1G_4$ ABSORPTION Pr^{3+}: $LiYF_4$

$^3H_4 \rightarrow {}^1G_4$

Line	Line frequency in vacuum (cm^{-1})	Polarization* and relative intensity	Temp (K)	S_4 symmetry assignment	Derived energy level for $^1G_4$ (cm^{-1})
1	9,620	90σ	30	$\Gamma_{3,4} \rightarrow \Gamma_1$	9,699
2	9,699	423π	10	$\Gamma_2 \rightarrow \Gamma_1$	9,699
3	9,753	45π	30	$\Gamma_{3,4} \rightarrow \Gamma_{3,4}$	9,832
4a	9,832	733σ	10	$\Gamma_2 \rightarrow \Gamma_{3,4}$	9,832
4b	9,832	18π	10	$\Gamma_2 \rightarrow \Gamma_{3,4}$†	9,832
5	10,112	1000σ	10	$\Gamma_2 \rightarrow \Gamma_{3,4}$	10,112
6	10,217	10π	10	$\Gamma_2 \rightarrow \Gamma_1$	10,217
7	10,313	41π	10	$\Gamma_2 \rightarrow \Gamma_1$	10,313

$^3P_0 \rightarrow {}^1G_4$

Line	Line frequency in vacuum (cm^{-1})	Polarization* and relative intensity	Temp (K)	S_4 symmetry assignment	Derived energy level for $^1G_4$ (cm^{-1})
1	11,026	301σ	10	$\Gamma_1 \rightarrow \Gamma_{3,4}$	9,832
2	10,930	1000π	10	$\Gamma_1 \rightarrow \Gamma_2$	9,930
3	10,849	647π	10	$\Gamma_1 \rightarrow \Gamma_2$	10,011

*π = polarized parallel to c-axis; σ polarized perpendicularly to c-axis.

†Tentatively identified as magnetic dipole transitions.

The $^1G_4$ multiplet splits into three Γ_1, two Γ_2, and two $\Gamma_{3,4}$ energy levels. From electric dipole selection rules for S_4 symmetry, we expect three π-polarized and two σ-polarized lines in the low temperature absorption spectrum. As shown in table XI, the expected three π lines (lines 2, 6, and 7) and two σ lines (lines 4a and 5) were observed in absorption at 10 K. At higher temperatures, absorption from the 79 cm^{-1} $\Gamma_{3,4}$ line in the $^3H_4$ multiplet is also expected to occur. At 30 K, one π-polarized line (line 3) and one σ-polarized line (line 1) were observed. These correspond to lines 2 and 4a, the two strongest low temperative absorption lines at 9699 and 9832 cm^{-1}. Line 4b is tentatively identified as a magnetic dipole transition.

Experimental energy levels of Pr^{3+} in YLF are listed in table XII for each multiplet studied. The irreducible representations are given in the table for both S_4 and D_2 site symmetries and were obtained from the calculations in section 5. Many low intensity or missing π transitions can be explained by considering the Pr^{3+} ion to be in an S_4 symmetry site that is nearly D_{2d}. Tables I and II show that π transitions between Γ_1 and Γ_2 states (S_4 notation) are allowed according to S_4 selection rules, but may be forbidden in D_{2d}. Table II shows that the Γ_1 level in S_4 notation corresponds to either the Γ_1 or the Γ_2 level in D_{2d}, and the Γ_2 level in S_4 corresponds to either the Γ_3 or the Γ_4 level in D_{2d}. According to D_{2d} selection rules, $\Gamma_1 \leftrightarrow \Gamma_4$ and $\Gamma_2 \leftrightarrow \Gamma_3$ transitions are allowed, but $\Gamma_1 \leftrightarrow \Gamma_3$ and $\Gamma_2 \leftrightarrow \Gamma_4$ transitions are forbidden. Figures 1 and 2 contain partial energy level diagrams for fluorescence transitions originating from the $^3P_0$ and $^1D_2$ levels, respectively.

The singlet $^3P_0$ level is Γ_1 for both S_4 and D_{2d} symmetries. The D_{2d} selection rules listed in figure 1 indicate that only half of the $\Gamma_1 \rightarrow \Gamma_2$ transitions (S_4 notation) in the $^3P_0$ fluorescence are allowed in D_{2d} symmetry. As shown in the figure, strong emission lines

were observed for all D_{2d} allowed transitions. For the most part, forbidden transitions either were not observed (lines c, k, and o) or were very weak (lines e, i, and n). The forbidden transitions a and g, which are comparable in intensity to the allowed transitions, are somewhat stronger than one might expect for forbidden transitions. Nevertheless, the use of D_{2d} selection rules is generally successful in explaining missing or weak lines in the $^3P_0$ fluorescence spectra.

TABLE XII. EXPERIMENTAL AND CALCULATED ENERGY LEVELS OF Pr^{3+}: LiYF$_4$

Multiplet	Experimental energy level (cm^{-1})	Calculated* energy level (cm^{-1})	S_4 site symmetry	D_{2d} site symmetry	$g_{\parallel}$
$^3H_4$	0	7	Γ_2	Γ_4	-
	79	84	$\Gamma_{3,4}$	Γ_5	-3.600
	-	217	Γ_1	Γ_1	-
	220	218	Γ_1	Γ_2	-
	496	487	$\Gamma_{3,4}$	Γ_5	0.170
	-	512	Γ_1	Γ_1	-
	-	514	Γ_2	Γ_3	-
$^3H_5$	2,253	2,255	Γ_1	Γ_2	-
	2,272	2,264	$\Gamma_{3,4}$	Γ_5	1.149
	2,280	2,285	Γ_2	Γ_3	-
	2,297	2,286	Γ_1	Γ_1	-
	2,341	2,336	$\Gamma_{3,4}$	Γ_5	4.908
	2,549	2,567	Γ_2	Γ_4	-
	- †	2,588	Γ_1	Γ_2	-
	- †	2,608	$\Gamma_{3,4}$	Γ_5	0.065
$^3H_6$	4,314	4,309	Γ_2	Γ_4	-
	4,394	4,409	$\Gamma_{3,4}$	Γ_5	1.617
	-	4,430	Γ_1	Γ_1	-
	-	4,458	Γ_2	Γ_3	-
	4,454	4,476	$\Gamma_{3,4}$	Γ_5	5.654
	4,486	4,511	Γ_1	Γ_2	-
	4,557	4,558	Γ_2	Γ_4	-
	-	4,879	Γ_1	Γ_1	-
	4,907	4,882	$\Gamma_{3,4}$	Γ_5	0.184
	4,945	4,926	Γ_2	Γ_3	-
$^3F_2$	-	5,159	Γ_1	Γ_1	-
	5,201	5,235	Γ_2	Γ_4	-
	5,221	5,218	$\Gamma_{3,4}$	Γ_5	0.789
	5,342	5,321	Γ_2	Γ_3	-

*See notes at end of table, p. 34.

TABLE XII. EXPERIMENTAL AND CALCULATED ENERGY LEVELS OF Pr^{3+}: $LiYF_4$ (Cont'd)

Multiplet	Experimental energy level (cm^{-1})	Calculated* energy level (cm^{-1})	S_4 site symmetry	D_{2d} site symmetry	$g_{\parallel}$
$^3F_3$	6,481	6,478	$\Gamma_{3,4}$	Γ_5	-0.433
	6,521	6,526	Γ_2	Γ_4	-
	6,586	6,562	Γ_1	Γ_2	-
	6,671	6,673	$\Gamma_{3,4}$	Γ_5	-4.596
	6,686	6,717	Γ_2	Γ_3	-
$^3F_4$	6,920	6,912	Γ_1	Γ_1	-
	6,942	6,919	$\Gamma_{3,4}$	Γ_5	-2.310
	6,983	6,957	Γ_2	Γ_4	-
	7,105	7,134	Γ_1	Γ_2	-
	7,116	7,123	Γ_2	Γ_3	-
	7,142	7,143	$\Gamma_{3,4}$	Γ_5	-1.226
	7,220	7,255	Γ_1	Γ_1	-
$^1G_4$	9,699	9,715	Γ_1	Γ_1	-
	9,832	9,815	$\Gamma_{3,4}$	Γ_5	-4.575
	9,930	9,931	Γ_2	Γ_4	-
	10,011	10,021	Γ_2	Γ_3	-
	10,112	10,170	$\Gamma_{3,4}$	Γ_5	0.228
	10,217	10,140	Γ_1	Γ_2	-
	10,313	10,592	Γ_1	Γ_1	-
$^1D_2$	16,740	16,868	Γ_2	Γ_3	-
	16,810	16,817	Γ_1	Γ_1	-
	17,083	17,080	$\Gamma_{3,4}$	Γ_5	2.121
	17,406	17,404	Γ_2	Γ_4	-
$^3P_0$	20,860	20,860	Γ_1	Γ_1	-
$^1I_6$	-	21,083	Γ_2	Γ_3	-
	-	21,084	Γ_2	Γ_4	-
	-	21,401	$\Gamma_{3,4}$	Γ_5	3.225
	-	21,414	Γ_1	Γ_1	-
	-	21,415	Γ_2	Γ_3	-
$^3P_1$	-	21,443	$\Gamma_{3,4}$	Γ_5	0.736
	-	21,611	Γ_1	Γ_2	-
$^1I_6$	-	21,622	$\Gamma_{3,4}$	Γ_5	7.514
	-	21,759	Γ_1	Γ_2	-
	-	22,033	Γ_1	Γ_1	-
	-	22,044	$\Gamma_{3,4}$	Γ_5	-2.279
	-	22,055	Γ_2	Γ_4	-
$^3P_2$	22,498‡	22,508	Γ_1	Γ_1	-
	22,645‡	22,636	$\Gamma_{3,4}$	Γ_5	2.663
	-	22,680	Γ_2	Γ_3	-

*See notes at end of table, p. 34.

TABLE XII. EXPERIMENTAL AND CALCULATED ENERGY LEVELS OF Pr^{3+}: $LiYF_4$ (Cont'd)

Multiplet	Experimental energy level (cm^{-1})	Calculated* energy level (cm^{-1})	S_4 site symmetry	D_{2d} site symmetry	$g_{\parallel}$
$^3P_2$	-	22,777	Γ_2	Γ_4	-
$^1S_0$	-	48,831	Γ_1	Γ_1	-

*Calculated from parameters of eq (4).

†Transitions to these levels were observed, but the lines are very broad. Hence, the energy levels (given in table V) are not included here.

‡These energies agree with those of H. H. Caspers and H. E. Rast, J. Luminescence, 10 (1975), 347.

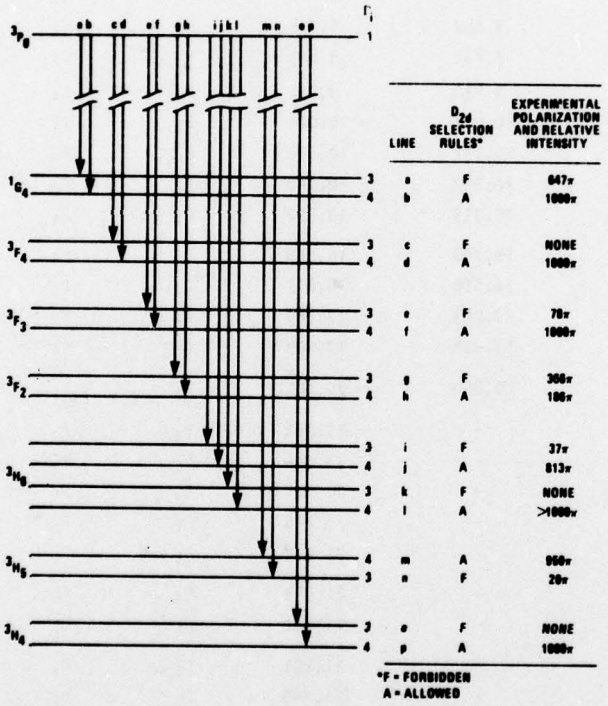

Figure 1. Partial energy level diagram (not to scale) showing $\Gamma_1 \rightarrow \Gamma_2$ transitions (S_4 notation) in $^3P_0$ fluorescence with D_{2d} representations for each level.

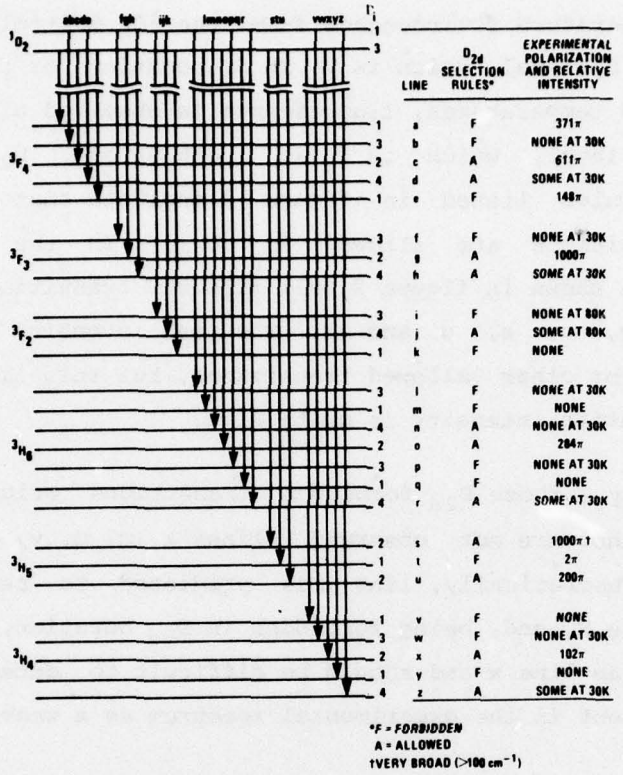

LINE	D_{2d} SELECTION RULES*	EXPERIMENTAL POLARIZATION AND RELATIVE INTENSITY
a	F	371π
b	F	NONE AT 30K
c	A	611π
d	A	SOME AT 30K
e	F	148π
f	F	NONE AT 30K
g	A	1000π
h	A	SOME AT 30K
i	F	NONE AT 80K
j	A	SOME AT 80K
k	F	NONE
l	F	NONE AT 30K
m	F	NONE
n	A	NONE AT 30K
o	A	284π
p	F	NONE AT 30K
q	F	NONE
r	A	SOME AT 30K
s	A	1000π†
t	F	2π
u	A	200π
v	F	NONE
w	F	NONE AT 30K
x	A	102π
y	F	NONE
z	A	SOME AT 30K

*F = FORBIDDEN
A = ALLOWED
†VERY BROAD (>100 cm^{-1})

Figure 2. Partial energy level diagram (not to scale) showing $\Gamma_1 \rightarrow \Gamma_2$ and $\Gamma_2 \rightarrow \Gamma_1$ transitions (S_4 notation) in $^1D_2$ fluorescence with D_{2d} representations for each level.

Low temperature fluorescence from the $^1D_2$ multiplet originates from the lowest $^1D_2$ level, which is Γ_2 in S_4 notation or Γ_3 in D_{2d} notation. At elevated temperatures, fluorescence is observed also from the next lowest $^1D_2$ level, which is Γ_1 in both S_4 and D_{2d} notations. The selection rules listed in figure 2 indicate that fewer than half of these transitions are allowed in D_{2d}. In the low temperature fluorescence shown in figure 2, all allowed transitions were observed (lines c, g, o, s, u, and x). The peak intensity for line s is much lower than for other allowed transitions, but this line is quite broad, and the relative intensity is quite high.

Generally, those D_{2d} forbidden transitions originating from the Γ_3 level either are not observed (lines k, m, q, v, and y) or are weak (line t). Theoretically, line y is predicted to be very close to the observed line x, and, being forbidden in D_{2d} notation, it is expected to be weaker than line x and should be difficult to detect. Hence, line y may be present in the experimental spectrum as a weak line superimposed on line x.

The forbidden D_{2d} lines a and e in the $^3F_4$ multiplet are weaker than the allowed line c in that multiplet. However, they are stronger than one might expect for forbidden transitions. At higher temperatures, transitions originating from the $^1D_2$ Γ_1 level also were observed. At 80 K, the allowed transition to the $^3F_2$ multiplet was observed, whereas the forbidden one was not. For the $^3H_4$, $^3F_3$, and $^3F_4$ multiplets at 30 K, all allowed transitions were observed and forbidden ones were not. The forbidden lines in the $^3F_3$ and $^3F_4$ fluorescences (lines b and f) were observed when the temperature was raised to 80 K.

Finally, the two forbidden transitions in the $^3H_6$ fluorescence were not observed at 30 K. However, only one of the two allowed transitions was observed. The other allowed transition (line n) apparently was weak and could not be identified because of background vibronic structure in this region of the spectrum.

The use of D_{2d} selection rules as a rule of thumb to explain missing or weak π transitions has succeeded here for Pr^{3+}:YLF. With few exceptions, π lines allowed in both D_2 and S_4 were observed and usually were quite strong. Those lines not allowed in D_{2d} were usually missing or quite weak. Many of the smaller π lines not expected in D_{2d} can be accounted for by small nonzero values of Im B_{64} and the odd-k B_{kq}.

5. CALCULATIONS

In previous work[23,24] a rationale was given for factoring the B_{kq} of the triply ionized lanthanide ions in a given host according to

$$B_{kq} = \rho_k A_{kq} \quad , \tag{9}$$

where ρ_k is a host independent term containing the electronic radial integrals and shielding factors, and the A_{kq} are impurity ion independent crystal field components obtained for a particular host by performing a lattice summation over the constituent ions. The ρ_k were given elsewhere[20] for the various rare earths so that approximate B_{kq} can be obtained for any of the lanthanide ions in a given host provided that B_{kq} have been determined for at least one of these ions in the host material. Preliminary values of the B_{kq} for Pr^{3+}:YLF were obtained earlier[21] by using the theoretical ρ_k to scale empirical

---

[20] *Clyde A. Morrison, Nick Karayianis, and Donald E. Wortman, Rare-Earth Ion-Host Lattice Interactions 4. Predicting Spectra and Intensities of Lanthanides in Crystals, Harry Diamond Laboratories TR-1816 (June 1977).*

[21] *D. E. Wortman, N. Karayianis, and C. A. Morrison, Rare-Earth Ion-Host Lattice Interactions 6. Lanthanides in $LiYF_4$, Harry Diamond Laboratories TR-1770 (August 1976).*

[23] *Nick Karayianis and Clyde A. Morrison, Rare-Earth Ion-Host Crystal Interactions 2. Local Distortion and Other Effects in Reconciling Lattice Sums and Phenomenological B_{km}, Harry Diamond Laboratories TR-1682 (January 1975).*

[24] *Richard P. Leavitt, Clyde A. Morrison, and Donald E. Wortman, Rare-Earth Ion-Host Crystal Interactions 3. Three-Parameter Theory of Crystal Fields, Harry Diamond Laboratories TR-1673 (June 1975).*

B_{kq} for Nd^{3+}:YLF. In the present work, this initial set of B_{kq} was varied in a least squares calculation (method 1), which used 36 energy levels in the multiplets $^3H_4$ through $^3P_0$. After use of the calculated levels to aid in establishing an energy level scheme for Pr^{3+} in YLF, the parameters in equation (1) were varied by using method 1 until a least-rms value of 15.8 cm^{-1} among 41 experimental and calculated energy levels was obtained. The B_{kq} yielding this fit are in units of cm^{-1}:

$$\begin{aligned} B_{20} &= 488.9 \pm 56 & B_{60} &= -42 \pm 115 \\ B_{40} &= -1043 \pm 140 & \text{Re } B_{64} &= 1213 \pm 58 \\ B_{44} &= 1242 \pm 93 & \text{Im } B_{64} &= 22.5 \pm 270 \end{aligned} \tag{10}$$

The ± values correspond to the amount that each B_{kq} would have to change to produce a shift of 15.8 cm^{-1} in the energy level most sensitive to that particular B_{kq}. These values were determined from the calculated derivatives of the energy levels with respect to the B_{kq}.

Using the same 41 energy levels that were used to obtain the above B_{kq}, we used also method 2, which diagonalizes the Hamiltonian given by equation (2) in a basis of states spanning the $4f^2$ configuration. The Hamiltonian given by equation (2) contains the Slater parameters, F_k; the spin-orbit parameter, ζ; the configuration interaction parameters, α, β, and γ; the Marvin integrals, M^k; and the crystal field parameters, B_{kq}. In the present calculation, γ was not varied since the electrostatic interaction is overspecified* without the $^1S_0$ multiplet and since it has the least effect on the L-S terms. The M^k were fixed at the Hartree-Fock ratios. We set Im B_{64} = 0 since the levels were not

*Data on states with differing seniority number v are necessary to specify γ uniquely. All multiplets except for $^1S_0$ ($v = 0$) have $v = 2$.

very sensitive to changes in it. New parameters that describe the Pr^{3+} free-ion interactions and new B_{kq} parameters that describe the perturbation by the crystal field on the free-ion levels were obtained. A least-rms value of 18 cm^{-1} between the experimental and calculated levels was obtained with the following parameters in units of cm^{-1} :

$$
\begin{array}{ll}
F_2 = 305.29 & M^0 = 2.1420 \\
F_4 = 46.379 & M^2 = 1.2013 \\
F_6 = 4.5173 & M^4 = 0.8155 \\
\zeta = 785.46 & B_{20} = 485 \\
\alpha = 23.451 & B_{40} = -1061 \\
\beta = -568.80 & B_{44} = 1296 \\
\gamma = 1342.9 & B_{60} = -57.5 \\
M_0^{(0)} = 4.7460 & B_{64} = 1186
\end{array}
\qquad (11)
$$

The B_{kq} obtained from either method 1 or method 2 do not differ appreciably, and their differences fall well within the uncertainties given for the B_{kq} in equation (10). In method 1, the aqua free-ion parameters[11] were used, and the centroids varied freely. The B_{kq} obtained by method 2, however, attempt to compensate for the fact that the free-ion parameters in equation (11) do not describe the energy centroids completely. For example, the experimental and calculated $^3P_0$ energy positions differ by 45 cm^{-1}, and a least-rms deviation of about 6 cm^{-1} was found among all the experimental and

[11] *W. T. Carnall, P. R. Fields, and K. J. Rajnak, J. Chem. Phys., 49 (1968), 4424.*

calculated energy centroids. Hence, the B_{kq} determined by method 1, in which the experimental and calculated energy centroids were matched, are preferred since the experimental crystal field splittings agree better with calculated ones. This result is not surprising since some interconfiguration interactions not considered have the same angular dependence[25] as those within the pure $4f^2$ configuration. These additional interactions are, therefore, lumped in with the latter in any empirical fit.

The experimental energy levels for the ground configuration of Pr^{3+} in YLF are given with the calculated levels in table XII; both S_4 and D_{2d} notations for the corresponding levels are given. The energy levels calculated for the ground term, ^3H, agree better with the experimental ones than do those for the higher terms. Most of the experimental and calculated ^3F levels also are consistent, but the calculations at the levels corresponding to 5201 and 5521 cm^{-1} are inverted, as are those corresponding to 7105 and 7116 cm^{-1}. Inversions occur also for the 10,112 and 10,217 cm^{-1} levels of $^1G_4$ and the 16,740 and 16,810 cm^{-1} levels of $^1D_2$. In addition, the experimental splitting of the $^1G_4$ multiplet was 614 cm^{-1}, whereas the calculated splitting was 877 cm^{-1}. For that reason, only the lower three energy levels of $^1G_4$ were used to obtain the best fit parameters given by equation (10). The 16,740-cm^{-1} energy level of $^1D_2$ also was left out of the calculation to determine the B_{kq} given in equation (10).

Next, a check was made to see whether the $^1G_4$ energy levels could be fit separately since, for this multiplet, the calculated splitting overestimates the experimental splitting by 50 percent. An rms deviation of 12 cm^{-1} resulted among six calculated and experimental

[25] *W. T. Carnall, H. Crosswhite, and H. M. Crosswhite, Energy Level Structure and Transition Probabilities of the Trivalent Lanthanides in LaF_3, Argonne National Laboratory, Chicago, IL (1978).*

$^1G_4$ energy levels. However, the energy levels for the other multiplets calculated with the $^1G_4$ B_{kq} did not agree with the experimental ones. Similar calculations were made for the ^3H and ^3F multiplets (table XIII). Since the higher energy levels[26] mix more strongly with the next higher electron configurations, the ground configuration wave functions might be expected to describe the ^3H and ^3F levels better than the ^1G, ^1D, and ^3P levels. Hence, the better agreement between calculated and experimental ^3H levels, for example, might be expected. In addition, the calculated $g_{||}$ factors for the doublet $\Gamma_{3,4}$ levels (table XII) require accurate wave functions and may be expected to be better for the lower lying levels partly because of configuration mixing.

TABLE XIII. PHENOMENOLOGICAL B_{kq} THAT FIT VARIOUS TERMS OF $4f^2$ CONFIGURATION FOR Pr^{3+}: LiYF$_4$

Term	B_{20}	B_{40}	B_{44}	B_{60}	Real B_{64}	Imaginary B_{64}	rms deviation (cm^{-1})	Levels (No.)
^3H	528	-1198	1318	-73	1245	99	10	17
^3H and ^3F	509	-1138	1268	-79	1212	-13	13	28
^1G	459	-253	925	-38	795	3	12	6
^3H through ^3P	489	-1043	1242	-42	1213	23	15.8	41

Note: Units are in cm^{-1}.

The even-k B_{kq} for Pr^{3+} in YLF, given in equation (10), are compared in table XIV with values obtained for Nd^{3+}, Ho^{3+}, Er^{3+}, and Tm^{3+} in YLF by the same theoretical model (method 1). As shown in the table, the magnitude of B_{kq} tends to decrease with increasing atomic number across the lanthanide series, in qualitative agreement with theoretical predictions.[20,24] Quantitatively, however, the phenomenological

[20] *Clyde A. Morrison, Nick Karayianis, and Donald E. Wortman, Rare-Earth Ion-Host Lattice Interactions 4. Predicting Spectra and Intensities of Lanthanides in Crystals, Harry Diamond Laboratories TR-1816 (June 1977).*

[24] *Richard P. Leavitt, Clyde A. Morrison, and Donald E. Wortman, Rare-Earth Ion-Host Crystal Interactions 3. Three-Parameter Theory of Crystal Fields, Harry Diamond Laboratories TR-1673 (June 1975).*

[26] *J. C. Morrison, P. R. Fields, and W. R. Carnall, Phys. Rev. B, 2 (1970), 3526.*

B_{kq} for YLF do not vary precisely as predicted by equation (9) with the ρ_k calculated by Wortman.[21] It has been suggested[24] that the agreement could be improved by incorporating effects such as wave function overlap in the calculation of ρ_k. Another possible reason for the discrepancy is the experimental uncertainty in B_{kq}. The uncertainty limits given in equation (10) for Pr^{3+} illustrate that some of the energy levels are relatively insensitive to B_{kq}. Consequently, somewhat different B_{kq} may be used without significantly changing the energy levels. In addition, the failure of the theory to accurately describe free-ion levels may introduce further uncertainty in the B_{kq}.

TABLE XIV. CRYSTAL FIELD PARAMETERS FOR TRIPLY IONIZED RARE EARTHS IN $LiYF_4$

Parameter	Pr^{3+}	Nd^{3+}*	Ho^{3+}†	Er^{3+}*	Tm^{3+}‡
B_{20}	489	441	410	400	333
B_{40}	-1043	-906	-615	-692	-648
B_{44}	1242	1114	819	925	876
B_{60}	-42	-26	-28	-21	-141
Real B_{64}	1213	1072	677	610	623
Imaginary B_{64}	23	21	33	149	3
rms deviation (cm^{-1})	15.8	3.5	2.8	4.1	7.5
Levels in fit (No.)	41	26	66	26	44

Note: Units are in cm^{-1}.

**From D. E. Wortman et al, HDL TR-1770 (August 1976).*
†From N. Karayianis et al, J. Phys. Chem. Solids, 37 (1976), 675.
‡R. P. Leavitt refit the experimental levels reported by H. P. Jenssen et al (Phys. Rev. B, 11 (1975), 92) using method 1, in which the calculated free-ion centroids were adjusted to fit the experimental centroids.

[21] *D. E. Wortman, N. Karayianis, and C. A. Morrison, Rare-Earth Ion-Host Lattice Interactions 6. Lanthanides in $LiYF_4$, Harry Diamond Laboratories TR-1770 (August 1976).*

[24] *Richard P. Leavitt, Clyde A. Morrison, and Donald E. Wortman, Rare-Earth Ion-Host Crystal Interactions 3. Three-Parameter Theory of Crystal Fields, Harry Diamond Laboratories TR-1673 (June 1975).*

Table XIV also lists the number of levels used in the fit to obtain the B_{kq} and the rms deviation for each of the five ions. An rms deviation of 15.8 cm^{-1} among 41 calculated and experimental energy levels for Pr^{3+} in YLF is somewhat larger than the rms values found for the other rare earths in YLF. For approximately the same number of levels, an rms deviation of 7.5 cm^{-1} is obtained for Tm^{3+}, which has a complementary electronic configuration to Pr^{3+} ($4f^{12}$ is treated like $4f^2$). In YLF, the crystal field splittings for Tm^{3+} are generally not so large as for Pr^{3+}. For example, the splitting of the $^3F_3$ multiplet for Tm^{3+} is 85 cm^{-1} compared with 205 cm^{-1} for Pr^{3+}. Such a comparison suggests that the Pr^{3+} fit is comparable with the Tm^{3+} fit. The calculated energy levels of $^1G_4$ and $^1D_2$ in Tm^{3+} are, as in Pr^{3+}, not in good agreement with experimental levels. For both of these ions, the energy levels used in the fitting procedures cover an energy range that includes all but the $^1S_0$ level.

Since these energy levels are not far from levels of higher electronic configurations, interconfiguration mixing may be a problem. For Nd^{3+}, Ho^{3+}, and Er^{3+}, the rms deviations of 3.5, 2.8, and 4.1 cm^{-1} are significantly lower than that for Pr^{3+}. Configurational mixing appears not too severe for these rare earths since the energy levels used in fitting are relatively far in energy from higher configuration levels. For example, for Nd^{3+}, only the ^4I term, whose energy levels are below 6500 cm^{-1}, is included in the fit.

When higher levels also are used, the agreement is not so good.[21] As shown in table XIII, when only the ^3H levels of Pr^{3+} are used in fitting, the rms deviation is reduced from 15.8 to 10 cm^{-1}. This, however, is still appreciably higher than the rms value for Nd^{3+}, which is next to Pr^{3+} in the lanthanide series. As anticipated, this

[21] *D. E. Wortman, N. Karayianis, and C. A. Morrison, Rare-Earth Ion-Host Lattice Interactions 6. Lanthanides in $LiYF_4$, Harry Diamond Laboratories TR-1770 (August 1976).*

result suggests that interconfiguration mixing may be more important for Pr^{3+} than for Nd^{3+}.

Following the procedure described in section 2.2, individual line intensities were calculated for absorption transitions from the ground state of the $^3H_4$ multiplet and for transitions between the fluorescing $^3P_0$ and $^1D_2$ levels and lower lying energy levels. This is the first time that electric dipole transition strengths were calculated by using odd-k B_{kq} determined ahead of time from a point charge lattice sum. The experimental intensities were compared with calculated values. Table XV compares the $^3P_0 \rightarrow {}^3H_4$, $^3H_4 \rightarrow {}^1G_4$, and $^3H_4 \rightarrow {}^1D_2$ transitions. These results are typical for other transitions, as well.

TABLE XV. CALCULATED AND EXPERIMENTAL INTENSITIES OF $^3P_0 \rightarrow {}^3H_4$, $^3H_4 \rightarrow {}^1G_4$, AND $^3H_4 \rightarrow {}^1D_2$ TRANSITIONS AT 10 K

Fluorescence transition	Energy level (cm^{-1})	Experimental relative intensity*	Calculated relative intensity*
$^3P_0 \rightarrow {}^3H_4$	0	1000π	605π
	79	249σ	1000σ
	496	94σ	386σ
	514	-	53π
$^3H_4 \rightarrow {}^1G_4$	9,699	423π	1000π
	9,832	733σ	128σ
	10,112	1000σ	66σ
	10,217	10π	3π
	10,313	41π	600π
$^3H_4 \rightarrow {}^1D_2$	16,810	1000π	1000π
	17,083	797σ	784σ

**The strongest line of each set of transitions is normalized to 1000.*

Although the calculated intensities in table XV do not agree quantitatively with experimental ones, there is some qualitative agreement, as illustrated by the $^3P_0 \rightarrow {}^3H_4$ transitions. For a particular polarization (σ or π), calculation correctly predicts how the lines appear in the order of increasing strength. The $^3P_0 \rightarrow {}^3H_4$ (79 cm^{-1})σ transition is predicted to be 2.6 times stronger than the $^3P_0 \rightarrow {}^3H_4$ (496 cm^{-1})σ line, in agreement with the data. For π polarization calculation correctly predicts the $^3P_0 \rightarrow {}^3H_4$ (0 cm^{-1}) line to be much stronger than the $^3P_0 \rightarrow {}^3H_4$ (514 cm^{-1}) transition. However, the relative magnitudes of calculated intensities between π and σ lines are reversed.

Similar results are found for the $^3H_4 \rightarrow {}^1G_4$ transitions, in which the order of intensities of the π transitions is correctly predicted. Though the order of theoretical σ intensities does not agree with the data for $^3H_4 \rightarrow {}^1G_4$ transitions, both σ lines are predicted to be of nearly equal intensity, as are the experimental values. A probable reason for the discrepancies noted between calculation and experiment is that the ground configuration wave functions do not adequately describe levels of higher energy, such as the $^1G_4$ levels or those in the $^3P_0$ and $^1D_2$ fluorescing multiplets.

For $^3H_4 \rightarrow {}^1D_2$ absorption, calculation and experiment give almost an exact fit. This surprising quantitative agreement is considered somewhat fortuitous.

Interconfiguration mixing by the crystal field may need considering to get better agreement between calculated and experimental energy levels and line intensities. Other workers[26-28] have taken into account

---

[26] *J. C. Morrison, P. R. Fields, and W. R. Carnall, Phys. Rev. B, 2 (1970), 3526.*

[27] *E. Y. Wong, J. Chem. Phys., 38 (1963), 976.*

[28] *B. R. Judd, Phys. Rev. Lett., 39 (1977), 242.*

some of the interconfiguration effects on the $4f^2$ energy level structure. Judd[28] recently approximated some of the effects of interconfiguration mixing by introducing a two-electron operator that adds a correction to the even-k B_{kq}. He improved the fit of the $^1D_2$ levels for Pr^{3+} in $LaCl_3$. His correction also is of the correct sign to improve the fit of the $^1D_2$ levels for Pr^{3+} in YLF, but it would further spread the calculated $^1G_4$ splitting, which is already too large. In a more complete treatment, Morrison et al[26] introduced two-electron operators that represent the excitation of a 4f electron to a higher-lying p or f orbital by means of the Coulomb interaction. This changed the even-k B by a small, but significant, amount. They improved the fit between the calculated and experimental $^1D_2$ levels for Pr^{3+} in $LaCl_3$ and improved the overall fit of the $4f^2$ levels by about 3 cm^{-1}. The above studies and the work described in this paper suggest that further consideration of interconfiguration mixing for Pr^{3+} in YLF may resolve some of the above discrepancies noted in the energy level calculations.

In this and previous* works, the intensities of transitions between Stark levels have been calculated by using perturbation theory to include the effect of mixing of opposite parity configurations by the odd-k B_{kq}. However, in Pr^{3+}, the higher configurations of opposite parity lie relatively close to the ground configuration, and therefore the perturbation approach may not be adequate. This difficulty may be circumvented by diagonalizing the $4f^2$, 4f5d, 4f6s, and 4f5g configurations simultaneously and fitting levels calculated in this way to experimental energy levels. The individual line intensites may then be calculated without resort to perturbation theory. Discrepancies found in this work between calculated and experimental intensities for Pr^{3+}:YLF might be resolved by including the effect of the odd-k B_{kq} interaction in this manner.

---

[26] *J. C. Morrison, P. R. Fields, and W. R. Carnall, Phys. Rev. B, 2 (1970), 3526.*

[28] *B. R. Judd, Phys. Rev. Lett., 39 (1977), 242.*

**See Selected Bibliography--Line Intensities.*

6. CONCLUSIONS

Energy levels for the $4f^2$ ground configuration of Pr^{3+} in YLF were established from high resolution absorption and fluorescence spectra. Energy level assignments were made assuming electric dipole transition selection rules for S_4 site symmetry. The wide band gap of YLF enabled spectral measurements to be made for all terms in the ground configuration except for the $^1S_0$ singlet level. From these measurements, 46 energy levels were established, including 44 in the lowest nine multiplets. Two methods were used in calculating energy levels. In method 1, the Pr^{3+} free-ion parameters and the B_{kq} were varied simultaneously to fit the experimental energy levels. The B_{kq} derived in this way attempted to compensate for the fact that the calculated energy centroids did not agree with experiment. Method 2 used free-ion parameters for Pr^{3+} in aqueous solutions, but allowed the energy centroids to vary freely in the calculation. The B_{kq} obtained from the latter approach were preferred since calculated energy levels agreed better with experimental ones. The B_{kq} determined gave an rms deviation of 15.8 cm^{-1} among 41 of the calculated and experimental energy values. These parameters were then used to obtain the remaining energy levels, yielding a complete energy level scheme for the $4f^2$ configuration of Pr^{3+}. Calculated and experimental energy levels agreed better for the lower terms than for the higher terms. Even-k B_{kq} parameters for Pr^{3+}:YLF were compared with values obtained for Nd^{3+}, Ho^{3+}, Er^{3+}, and Tm^{3+} by using the same theoretical model. The values of B_{kq} decreased with atomic number for the lanthanide series, but not precisely as predicted by theory.

In the analysis of the experimental data, D_{2d} electric dipole selection rules also were considered to explain missing or weak transitions that are allowed in S_4. Generally, π lines that are allowed in both D_{2d} and S_4 notations were observed and were quite strong. Those π transitions allowed in S_4 but forbidden in D_{2d} were usually

missing or quite weak. Hence, the use of D_{2d} selection rules has been a useful rule of thumb in identifying energy levels and explaining weak or missing transitions in Pr^{3+}:YLF.

Electric dipole transition strengths were determined by using odd-k B_{kq} calculated ahead of time from a lattice sum. The calculated intensities agreed qualitatively with experimental ones. Generally, the theory predicts the correct order of intensities for transitions of a particular polarization. However, predictions of the relative line strengths within a given polarization and the relative intensities between the two polarizations are unreliable.

Future work will focus on refinements of the crystal field theory to improve predictions of energy levels and line strengths. Inclusion of configuration interaction by using an approach similar to that of Morrison et al[26] should remove some of the discrepancies in the energy level calculation by improving the even-k B_{kq}. Explicit consideration of opposite parity configurations as described in this work will affect the odd-k B_{kq} and may improve the agreement between calculated and experimental intensities.

---

[26] *J. C. Morrison, P. R. Fields, and W. R. Carnall, Phys. Rev. B, 2 (1970), 3526.*

LITERATURE CITED

(1) H.P. Jenssen, Phonon Assisted Laser Transitions and Energy Transfer in Rare Earth Laser Crystals, Massachusetts Institute of Technology Crystal Physics Laboratory, Cambridge, MA, Technical Report 16 (September 1971).

(2) H. H. Caspers and H. E. Rast, J. Luminescence, 10 (1975), 347.

(3) N. Karayianis, D. E. Wortman, and H. P. Jenssen, J. Phys. Chem. Solids, 37 (1976), 675.

(4) H. P. Jenssen, A. Linz, R. P. Leavitt, C. A. Morrison, and D. E. Wortman, Phys. Rev. B, 11 (1975), 92.

(5) W. Heaps, L. R. Elias, and W. M. Yen, Phys. Rev. B, 13 (1975), 94.

(6) K. Rajnak and B. G. Wybourne, J. Chem. Phys., 41 (1964), 565.

(7) L. Esterowitz, R. Allen, M. Kruer, F. Bartoli, L. S. Goldberg, H. P. Jenssen, A. Linz, and V. O. Nicolai, J. Appl. Phys., 48 (1977), 650.

(8) E. P. Chicklis, C. S. Naiman, R. C. Folweiler, D. R. Gabbe, H. P. Jenssen, and A. Linz, Appl. Phys. Lett., 19 (1971), 119.

(9) M. J. Weber in Handbook of Lasers, R. J. Presseley, ed., The Chemical Rubber Co., Cleveland, OH (1971).

(10) B. G. Wybourne, Spectroscopic Properties of Rare Earths, John Wiley and Sons, Inc., New York (1965).

(11) W. T. Carnall, P. R. Fields, and K. J. Rajnak, J. Chem. Phys., 49 (1968), 4424.

(12) J. S. Margolis, J. Chem. Phys., 35 (1961), 1367.

(13) B. R. Judd, Operator Techniques in Atomic Spectroscopy, McGraw-Hill Book Co., New York (1963).

(14) K. Rajnak and B. G. Wybourne, Phys. Rev., 132 (1963), 280.

(15) B. R. Judd, Phys. Rev., 127 (1962), 750.

(16) G. S. Ofelt, J. Chem. Phys., 37 (1962), 511.

(17) E. U. Condon and G. H. Shortley, The Theory of Atomic Spectra, Cambridge University Press, Cambridge, U.K. (1959).

(18) P. Grossgut, Doctoral Dissertation, Texas Christian University (1971); University Microfilms, Ann Arbor, MI, No. 72-7621.

(19) A. J. Freeman and R. E. Watson, Phys. Rev., 127 (1962), 2058.

(20) Clyde A. Morrison, Nick Karayianis, and Donald E. Wortman, Rare-Earth Ion-Host Lattice Interactions 4. Predicting Spectra and Intensities of Lanthanides in Crystals, Harry Diamond Laboratories TR-1816 (June 1977).

(21) D. E. Wortman, N. Karayianis, and C. A. Morrison, Rare-Earth Ion-Host Lattice Interactions 6. Lanthanides in $LiYF_4$, Harry Diamond Laboratories TR-1770 (August 1976).

(22) G. F. Koster, J. O. Dimmock, R. G. Wheeler, and H. Statz, Properties of the Thirty-Two Point Groups, MIT Press, Cambridge, MA (1963).

(23) Nick Karayianis and Clyde A. Morrison, Rare-Earth Ion-Host Crystal Interactions 2. Local Distortion and Other Effects in Reconciling Lattice Sums and Phenomenological B_{km}, Harry Diamond Laboratories TR-1682 (January 1975).

(24) Richard P. Leavitt, Clyde A. Morrison, and Donald E. Wortman, Rare-Earth Ion-Host Crystal Interactions 3. Three-Parameter Theory of Crystal Fields, Harry Diamond Laboratories TR-1673 (June 1975).

(25) W. T. Carnall, H. Crosswhite, and H. M. Crosswhite, Energy Level Structure and Transition Probabilities of the Trivalent Lanthanides in LaF_3, Argonne National Laboratory, Chicago, IL (1978).

(26) J. C. Morrison, P. R. Fields, and W. R. Carnall, Phys. Rev. B, 2 (1970), 3526.

(27) E. Y. Wong, J. Chem. Phys., 38 (1963), 976.

(28) B. R. Judd, Phys. Rev. Lett., 39 (1977), 242.

SELECTED BIBLIOGRAPHY

Energy Level Structure

Carnall, W. T., Crosswhite, H., Crosswhite, H. M., and Conway, J. G., J. Chem. Phys, 64 (1976), 3582.

Crosswhite, H. M., Spectroscopie des Éléments de Transition et des Éléments Lourds dans les Solides, Colloques Internationaux, C.N.R.S., Lyon, No. 255 (1976), 65.

Crosswhite, H. M., Crosswhite, H., Edelstein, N., and Rajnak, K., J. Chem. Phys.,67 (1977), 3002.

Crosswhite, H. M., Crosswhite, H., Kaseta, F. W., and Sarup, R., J. Chem. Phys., 64 (1976), 1981.

Energy Levels of Rare-Earth Ions in YLF

Brown, M. R., Roots, K. G., and Shand, W. A., J. Phys. C, 2 (1969), 593.

Line Intensities for Rare-Earth Ions

Axe, J. D., Jr., J. Chem. Phys., 39 (1963), 1154.

Becker, B.J., Phys. Stat. Sol. B, 43 (1971), 583.

Delsart, C. and Pelletier-Allard, N., J. Phys. (Paris), 32 (1971), 507; J. Phys. C, 6 (1973), 1277.

Porcher, P., and Caro, P., J. Chem. Phys., 68 (1978), 4176; J. Chem. Phys., 68 (1978), 4183.

Multiplet-to-Multiplet Intensities

Caird, J. A., On the Evaluation of Rare Earth Laser Materials and the Matrix Elements of Orbital Tensor Operators, Air Force Avionics Laboratory TR-73-323 (October 1973).

Weber, M. J., Varitimos, T. E., and Matzinger, B. H., Optical Intensities of Rare Earth Ions in Yttrium Orthoaluminate, Phy. Rev. B, 8 (July 1973), 47-53.

Multiplet-to-Multiplet Intensities for Nd^{3+} Ion

Lomheim, T. S., and DeShazer, L. G., Opt. Comm., 24 (1978), 89.

SELECTED BIBLIOGRAPHY (Cont'd)

Multiplet-to-Multiplet Intensities for Pr^{3+} Ion

Carnall, W. T., Fields, P. R., and Wybourne, B. G., J. Chem. Phys., 42 (1965), 3797.

Krupke, W. F., Phys. Rev., 145 (1966), 325.

Weber, M. J., J. Chem. Phys., 48 (1968), 4771; Phys, Rev., 171 (1968), 283.

DISTRIBUTION

DIRECTOR
DEFENSE COMMUNICATIONS ENGINEER CENTER
1860 WIEHLE AVE
RESTON, VA 22090
ATTN PETER A. VENA

COMMANDER
US ARMY MISSILE RESEARCH
& DEVELOPMENT COMMAND
REDSTONE ARSENAL, AL 35809
ATTN DRDMI-TB, REDSTONE SCI INFO CENTER
ATTN DRCPM-HEL, DR. W. B. JENNINGS
ATTN DR. J. P. HALLOWES
ATTN T. HONEYCUTT

COMMANDER
EDGEWOOD ARSENAL
EDGEWOOD ARSENAL, MD 21010
ATTN SAREA-TS-L, TECH LIBRARY

COMMANDER
US ARMY ARMAMENT RES & DEV COMMAND
DOVER, NJ 07801
ATTN DRDAR-TSS, STINFO DIV

COMMANDER
USA TEST & EVALUATION COMMAND
ABERDEEN PROVING GROUND, MD 21005
ATTN TECH LIBRARY

COMMANDER
USA ABERDEEN PROVING GROUND
ABERDEEN PROVING GROUND, MD 21005
ATTN STEAP-TL, TECH LIBRARY, BLDG 305

COMMANDER
WHITE SANDS MISSILE RANGE, NM 88002
ATTN DRSEL-WL-MS, ROBERT NELSON

COMMANDER
GENERAL THOMAS J. RODMAN LABORATORY
ROCK ISLAND ARSENAL
ROCK ISLAND, IL 61201
ATTN SWERR-PL, TECH LIBRARY

COMMANDER
USA CHEMICAL CENTER & SCHOOL
FORT MC CLELLAN, AL 36201

COMMANDER
NAVAL OCEAN SYSTEMS CENTER
SAN DIEGO, CA 92152
ATTN TECH LIBRARY

COMMANDER
NAVAL SURFACE WEAPONS CENTER
WHITE OAK, MD 20910
ATTN WX-40, TECHNICAL LIBRARY

DIRECTOR
NAVAL RESEARCH LABORATORY
WASHINGTON, DC 20390
ATTN CODE 2620, TECH LIBRARY BR
ATTN CODE 5554,
DR. LEON ESTEROWITZ (10 COPIES)
ATTN CODE 5554,
DR. S. BARTOLI (10 COPIES)
ATTN CODE 5554, R. E. ALLEN (10 COPIES)

COMMANDER
NAVAL WEAPONS CENTER
CHINA LAKE, CA 93555
ATTN CODE 753, LIBRARY DIV

COMMANDER
AF ELECTRONICS SYSTEMS DIV
L. G. HANSCOM AFB, MA 01730
ATTN TECH LIBRARY

DEPARTMENT OF COMMERCE
NATIONAL BUREAU OF STANDARDS
WASHINGTON, DC 20234
ATTN LIBRARY
ATTN DR. W. BROWNER
ATTN H. S. PARKER

DEPARTMENT OF COMMERCE
NATIONAL BUREAU OF STANDARDS
BOULDER, CO 80302
ATTN LIBRARY

DIRECTOR
LAWRENCE RADIATION LABORATORY
LIVERMORE, CA 94550
ATTN DR. MARVIN J. WEBER
ATTN DR. HELMUT A. KOEHLER

NASA GODDARD SPACE FLIGHT CENTER
GREENBELT, MD 20771
ATTN CODE 252, DOC SECT, LIBRARY

NATIONAL OCEANIC & ATMOSPHERIC ADM
ENVIRONMENTAL RESEARCH LABORATORIES
BOULDER, CO 80302
ATTN LIBRARY, R-51, TECH REPORTS

CARNEGIE MELLON UNIVERSITY
SCHENLEY PARK
PITTSBURGH, PA 15213
ATTN PHYSICS & EE
DR. J. O. ARTMAN

UNIVERSITY OF MICHIGAN
COLLEGE OF ENGINEERING NORTH CAMPUS
DEPARTMENT OF NUCLEAR ENGINEERING
ANN ARBOR, MI 48104
ATTN DR. CHIHIRO KIKUCHI

DISTRIBUTION (Cont'd)

DEFENSE DOCUMENTATION CENTER
CAMERON STATION, BUILDING 5
ALEXANDRIA, VA 22314
ATTN DDC-TCA (12 COPIES)

COMMANDER
USA RSCH & STD GP (EUR)
BOX 65
FPO NEW YORK 09510
ATTN LTC JAMES M. KENNEDY, JR.
CHIEF, PHYSICS & MATH BRANCH

COMMANDER
US ARMY MATERIEL DEVELOPMENT
& READINESS COMMAND
5001 EISENHOWER AVENUE
ALEXANDRIA, VA 22333
ATTN DRXAM-TL, HQ TECH LIBRARY
ATTN DRCDE, DIR FOR DEV & ENGR
ATTN DRCDMD-ST

COMMANDER
US ARMY ARMAMENT MATERIEL
READINESS COMMAND
ROCK ISLAND ARSENAL
ROCK ISLAND, IL 61299
ATTN DRSAR-ASF, FUZE
& MUNITIONS SPT DIV
ATTN DRSAR-LEP-L, TECHNICAL LIBRARY

COMMANDER
USA MISSILE & MUNITIONS
CENTER & SCHOOL
REDSTONE ARSENAL, AL 35809
ATTN ATSK-CTD-F

DIRECTOR
US ARMY MATERIEL SYSTEMS
ANALYSIS ACTIVITY
ABERDEEN PROVING GROUND, MD 21005
ATTN DRXSY-MP

DIRECTOR
DEFENSE ADVANCED RESEARCH
PROJECTS AGENCY
ARCHITECT BLDG
1400 WILSON BLVD
ARLINGTON, VA 22209

DIRECTOR
DEFENSE NUCLEAR AGENCY
WASHINGTON, DC 20305
ATTN APTL, TECH LIBRARY

DIRECTOR OF DEFENSE RES AND
ENGINEERING
WASHINGTON, DC 20301
ATTN TECHNICAL LIBRARY (3C128)

OFFICE, CHIEF OF RESEARCH,
DEVELOPMENT, & ACQUISITION
DEPARTMENT OF THE ARMY
WASHINGTON, DC 20310
ATTN DAMA-ARZ-A, CHIEF SCIENTIST
DR. M. E. LASSER
ATTN DAMA-ARZ-B, DR. I. R. HERSHNER

COMMANDER
US ARMY RESEARCH OFFICE (DURHAM)
PO BOX 12211
RESEARCH TRIANGLE PARK, NC 27709
ATTN DR. ROBERT J. LONTZ
ATTN DR. CHARLES BOGOSIAN

COMMANDER
ARMY MATERIALS & MECHANICS RESEARCH
CENTER
WATERTOWN, MA 02172
ATTN DRXMR-TL, TECH LIBRARY BR

COMMANDER
NATICK LABORATORIES
NATICK, MA 01762
ATTN DRXRES-RTL, TECH LIBRARY

COMMANDER
USA FOREIGN SCIENCE & TECHNOLOGY CENTER
FEDERAL OFFICE BUILDING
220 7TH STREET NE
CHARLOTTESVILLE, VA 22901
ATTN DRXST-BS, BASIC SCIENCE DIV

DIRECTOR
USA BALLISTICS RESEARCH LABORATORIES
ABERDEEN PROVING GROUND, MD 21005
ATTN DRXBR, DIRECTOR, R. EICHELBERGER
ATTN DRXBR-TB, FRANK J. ALLEN
ATTN DRXBR, TECH LIBRARY
ATTN DRDAR-TSB-S (STINFO)

DIRECTOR
ELECTRONIC WARFARE LABORATORY
FT MONMOUTH, NJ 07703
ATTN J. CHARLTON
ATTN TECHNICAL LIBRARY
ATTN DR. HIESLMAIR
ATTN J. STROZYK
ATTN DR. E. J. TEBO

DIRECTOR
NIGHT VISION & ELECTRO-OPTICS LABORATORY
FT BELVOIR, VA 22060
ATTN TECHNICAL LIBRARY
ATTN R. BUSER

COMMANDER
ATMOSPHERIC SCIENCES LABORATORY
WHITE SANDS MISSILE RANGE, NM 88002
ATTN TECHNICAL LIBRARY

DISTRIBUTION (Cont'd)

DIRECTOR
ADVISORY GROUP ON ELECTRON DEVICES
201 VARICK STREET
NEW YORK, NY 10013
 ATTN SECTRY, WORKING GROUP D

OFFICE OF NAVAL RESEARCH
ARLINGTON, VA 22217
 ATTN DR. V. O. NICOLAI

US ARMY ELECTRONICS RESEARCH
 & DEVELOPMENT COMMAND
 ATTN WISEMAN, ROBERT S., DR., DRDEL-CT
 ATTN PAO

HARRY DIAMOND LABORATORIES
 ATTN 00100, COMMANDER/TECHNICAL DIR/TSO
 ATTN CHIEF, 00210
 ATTN CHIEF, DIV 10000
 ATTN CHIEF, DIV 20000
 ATTN CHIEF, DIV 30000
 ATTN CHIEF, DIV 40000
 ATTN CHIEF, LAB 11000
 ATTN CHIEF, LAB 13000
 ATTN CHIEF, LAB 15000
 ATTN CHIEF, LAB 22000
 ATTN CHIEF, LAB 21000
 ATTN CHIEF, LAB 34000
 ATTN CHIEF, LAB 36000
 ATTN CHIEF, LAB 47000
 ATTN CHIEF, LAB 48000
 ATTN RECORD COPY, 94100
 ATTN HDL LIBRARY, 41000 (5 COPIES)
 ATTN HDL LIBRARY, 41000 (WOODBRIDGE)
 ATTN CHAIRMAN, EDITORIAL COMMITTEE
 ATTN TECHNICAL REPORTS BRANCH, 41300
 ATTN LEGAL OFFICE, 97000
 ATTN LANHAM, C., 00210
 ATTN WILLIS, B., 47400
 ATTN FARRAR, R., 13500
 ATTN GLEASON, T., 15400
 ATTN KARAYIANIS, N., 13200 (10 COPIES)
 ATTN KULPA, S., 13200
 ATTN LEAVITT, R., 13200 (10 COPIES)
 ATTN MORRISON, C., 13200 (10 COPIES)
 ATTN NEMARICH, J., 11130
 ATTN SCALES, J. III, 15400
 ATTN WORTMAN, D., 13200 (10 COPIES)
 ATTN SATTLER, J., 13200
 ATTN WEBER, B., 13200
 ATTN SIMONIS, G., 13200
 ATTN WORCHESKY, T., 13200